Cooling histories of mountain ranges in the southern Rio Grande rift based on apatite fission-track analysis--A reconnaissance survey

Shari A. Kelley and Charles E. Chapin

New Mexico Geology, v. 19, n. 1 pp. 1-14, Print ISSN: 0196-948X, Online ISSN: 2837-6420.
https://doi.org/10.58799/NMG-v19n1.1

New Mexico Bureau of Geology & Mineral Resources
New Mexico Institute of Mining & Technology
801 Leroy Place
Socorro, NM 87801-4796

https://geoinfo.nmt.edu

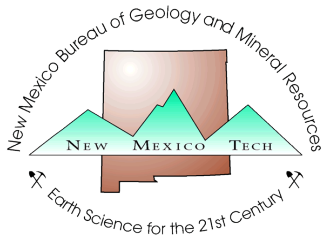

This page is intentionally left blank to maintain order of facing pages.

New Mexico GEOLOGY
• Science and Service
ISSN 0196-948X
Volume 19, No. 1, February 1997

Cooling histories of mountain ranges in the southern Rio Grande rift based on apatite fission-track analysis—a reconnaissance survey

by *Shari A. Kelley*, Dept. of Earth and Environmental Sciences, New Mexico Institute of Mining & Technology, Socorro, NM 87801-4796;
and *Charles E. Chapin*, New Mexico Bureau of Mines & Mineral Resources, Socorro, NM 87801-4796

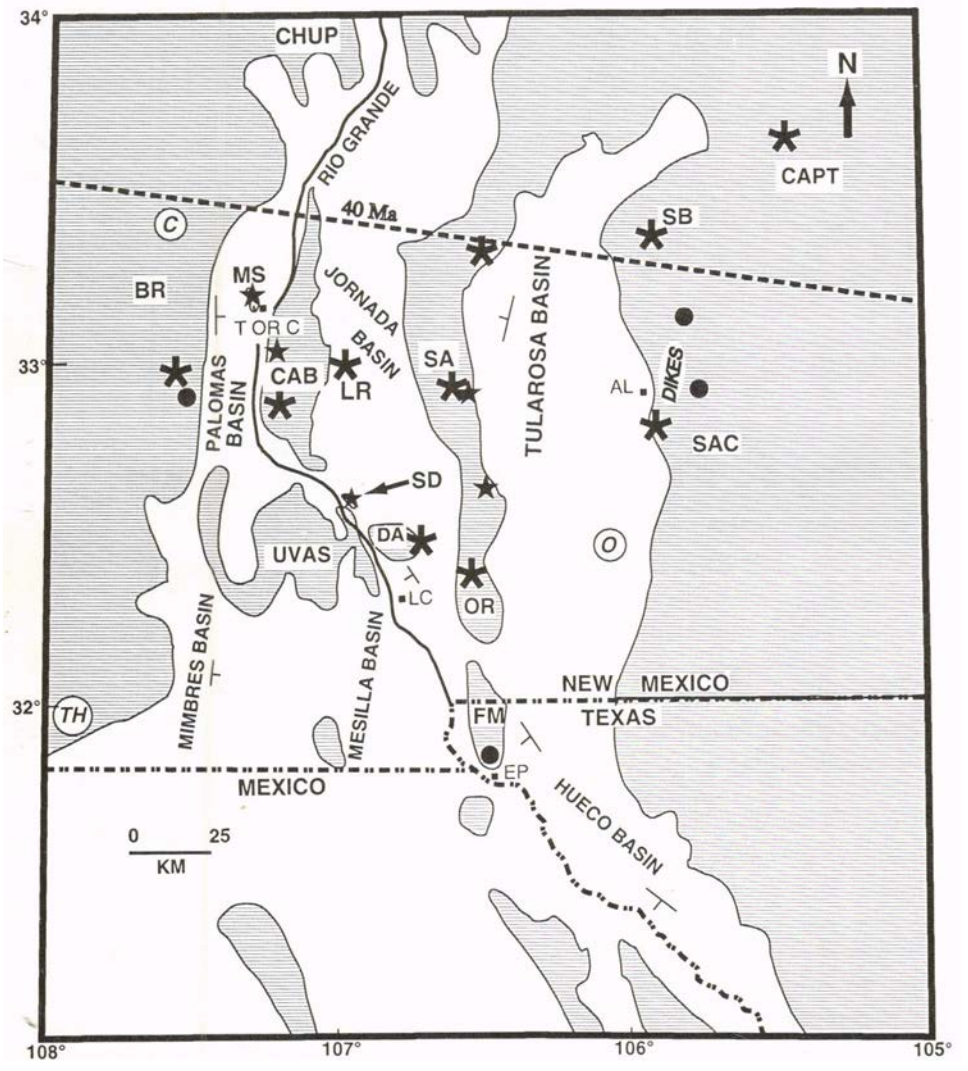

FIGURE 1—Regional location map for the southern Rio Grande rift; the rift basins are white and the mountain ranges and basins outside of the rift are shaded. The dominant dip of the half-grabens is shown with the strike-and-dip symbols. **SAC,** Sacramento Mountains; **SB,** Sierra Blanca; **CAPT,** Capitan Mountains; **SA,** San Andres Mountains; **OR,** Organ Mountains; **FM,** Franklin Mountains; **DA,** Doña Ana Mountains; **SD,** San Diego Mountain; **CAB,** Caballo Mountains; **MS,** Mud Springs Mountains; **UVAS,** Sierra de las Uvas; **CHUP,** Chupadera Mountains; BR, Black Range. Locations of Eocene dikes east of Alamogordo and Eocene intrusions discussed in this paper are in italics: **TH,** Tres Hermanos; *0,* Orogrande; *C,* Cuchillo. Dashed line shows northern extent of Eocene intrusives with ages older than 40 Ma. Cities and towns shown for reference are **AL,** Alamogordo; **EP,** El Paso; LC, **Las** Cruces; **T or C,** Truth or Consequences. General AFT age ranges are *, 0-10 Ma; *, 10-40 Ma; 0, >40 Ma.

Abstract

Fifty-two apatite fission-track (AFT) and two zircon fission-track ages were determined during a reconnaissance study of the cooling and tectonic history of uplifts associated with the southern Rio Grande rift in south-central New Mexico. Mack et al. (1994a, b) proposed that the southern rift has been affected by four episodes of extension beginning at about 35 Ma. The main phases of faulting started in the late Eocene, the late Oligocene, the middle Miocene, and the latest Miocene to early Pliocene, with each phase disrupting earlier rift basins and in some cases reversing the dip of the early rift half-grabens found in the vicinity of the southern Caballo Mountains. The timing of denudation derived from AFT data in the Caballo, Mud Springs, San Diego, and Dona Ana mountains are consistent with the episodes of uplift and erosion preserved in the Oligocene to Miocene Hayner Ranch and Rincon Valley Formations in the southern Caballo Mountains.

Each mountain block studied in the southern rift has a unique history. AFT ages in the Proterozoic rocks on the east side of the San Andres Mountains record cooling of this mountain block at 21 to 22 Ma in response to the phase of extension that began in the late Oligocene. Younger AFT ages of 7 to 8 Ma related to the middle Miocene

Also in this issue

Coming soon

The first 100 years of the New Mexico Mineral Museum
Triassic stratigraphy and paleontology on the Ft. Wingate quadrangle

episode of extension are exposed on the upthrown side of high-angle faults cutting the Proterozoic rocks. AFT ages from the eastern Organ Mountains are 10-17 Ma and the mean track lengths are long; the ages on the west side are 20-29 Ma and the mean track lengths are shorter. A westward-tilted partial-annealing zone for apatite that formed during protracted cooling of the Organ batholith in the late Oligocene to early Miocene is preserved in this mountain block. Rapid denudation (200-400 m/m.y.) and tilting of the range occurred in the middle Miocene. The base of a poorly defined apatite partial-annealing zone that formed during burial of southern New Mexico in the Mesozoic is preserved in the Sacramento Mountains. The earliest phase of extension is recorded in the AFT data from Proterozoic rocks exposed at the base of the Sacramento escarpment. Evidence for significant denudation related to Laramide deformation or late Oligocene and middle Miocene extension is not observed in the AFT data from the Sacramento Mountains. AFT data derived from samples in Oligocene to Miocene intrusions (Capitan, Sierra Blanca, and Black Range) record rapid cooling of these shallowly emplaced plutons.

The AFT data from the northern and southern Rio Grande rift are similar in many respects. The trend of young AFT ages and greater denudation on footwall blocks adjacent to the master faults controlling the geometry of the half-grabens that was observed in northern New Mexico is also found in southern New Mexico. Horst blocks in the rift that are bordered by normal faults on two or three sides invariably have young (<12 Ma) AFT ages and high (>10°C /Ma) cooling rates. In the places where Mesozoic AFT ages are preserved, the estimated cooling rates are low (<2°C /Ma) in both the northern and southern rift. The primary difference in the cooling histories of mountain ranges in the northern and southern rift is the paucity of AFT ages that are older than 30 Ma in the southern rift. Part of this trend may be a function of sampling bias.

Zircon FT and K-Ar data are used to examine the distribution of late Mesozoic to Eocene volcanism in southern New Mexico. A previously unrecognized Cretaceous intrusion was identified southeast of Hillsboro using zircon FT dating. The porphyry from this intrusion was the source of volcanic clasts in the Late Cretaceous to early Tertiary McRae Formation in the northeastern Caballo Mountains. In addition, a zircon FT age of 49.6 ±3.8 Ma for the rhyolite sill capping Salinas Peak at the north end of the San Andres Mountains and K-Ar ages for the Orogrande, Cuchillo, and Tres Hermanos stocks are used to constrain the northern limit of 40 Ma volcanism in south-central New Mexico.

Introduction

Recently, detailed geologic mapping and stratigraphic studies by Seager et al. (1984), Seager and Mack (1986), Mack and Seager (1990), and Mack et al. (1994 a, b) have constrained the timing and orientation of Cenozoic compressive and extensional events that affected the mountain ranges of the southern Rio Grande rift near Las Cruces, New Mexico. First, Paleogene Laramide compression formed west-northwest-trending basement uplifts bounded by southwest-dipping, high-angle reverse faults (Seager and Mack, 1986; Seager et al., 1986). This compressional phase occurred mainly in the Paleocene to early Eocene, although there is evidence for deformation as early as Late Cretaceous and as late as late Eocene. Following Laramide deformation, regional calc-alkaline volcanism during the latest Eocene to Oligocene blanketed large portions of southern New Mexico with layers of ash-flow tuff, suggesting that the topographic relief by the middle Oligocene was not as large as it is today. Volcanism was followed by, and was in part coeval with, extension, leading to the development of the Rio Grande rift, a north-trending continental rift that extends from northern Colorado to northern Mexico. On the basis of the analysis of sedimentary deposits in the southern Caballo Mountains, Dona Ana Mountains, San Diego Mountain, and Sierra de las Uvas (Fig. 1), Mack et al. (1994a, b) proposed that the southern rift has been affected by four episodes of extension beginning at about 35 Ma. The main phases of faulting started in the late Eocene, the late Oligocene, the middle Miocene, and the latest Miocene to early Pliocene, with each phase disrupting earlier rift basins and in some cases reversing the dip of the early rift half-grabens [Note: The Eocene-Oligocene boundary used in this paper is approximately 33-34 Ma as documented by Swisher and Prothero (1990) and McIntosh et al. (1992b)].

The nature of the early episodes of rift extension outside of the area studied by Mack et al. (1994a, b) is not well known because much of the early Miocene to Oligocene extensional history of the southern rift is buried beneath younger deposits (Clemons and Osburn, 1986). Consequently, other techniques must be used to locate areas affected by early extension and to understand the timing and the amount of denudation associated with these stages of deformation. An approach that gives spatial and temporal data on the development of vertical relief associated with rift formation involves determining the cooling history of rocks in mountain ranges that bound the rift using apatite fission-track (AFT) analysis (Green et al., 1989). Fission-track annealing in apatite is controlled primarily by temperature and the chemical composition of the apatite (tracks in chlorapatite completely anneal at higher temperatures (140°C) than those in fluorapatite (120°C); Green et al., 1986; Green, oral comm. 1996). In a relatively stable geological environment where temperatures as a function of depth are now at a maximum, apatite fission-track (AFT) age and track lengths decrease systematically with depth (Naeser, 1979; Fitzgerald et al., 1995). At temperatures less than 60 to 70°C, tracks that are produced by the spontaneous fission of ^{238}U are retained and annealing is relatively minor. The AFT ages of detrital grains in sedimentary rocks at shallow depths (temperatures <70°C) are equivalent to or greater than the stratigraphic age of the rock unit and the mean track lengths are on the order of 13 to 15 µm. The AFT ages in basement rocks at shallow depth (temperatures <70°C) would reflect the cooling history of the basement prior to the period of stability, and, as with sedimentary rocks, the mean track lengths would be relatively long (>13 µm). In the temperature range known as the partial-annealing zone (PAZ), which is between 60-70°C and 120-140°C, depending on the composition of the apatite, the AFT ages and track lengths are reduced compared to the original AFT ages and lengths. Mean track lengths in the PAZ are typically 8 to 13

New Mexico GEOLOGY

• Science and Service

ISSN 0196-948X

Volume 19, No. 1, February 1997

Editor: Carol A. Hjellming

EDITORIAL BOARD

Steve M. Cather, *NMBMMR*, Chairman
Thomas Giordano, *NMSU*
Laurel B. Goodwin, *NMIMT*
Spencer G. Lucas, *NMMNHS*
Frank J. Pazzaglia, *UNM*

Published quarterly by
New Mexico Bureau of Mines and Mineral Resources
a division of New Mexico Institute of Mining and Technology

BOARD OF REGENTS

Ex-Officio
Gary Johnson, *Governor of New Mexico*
Alan Morgan, *Superintendent of Public Instruction*
Appointed
J. Michael Kelly, *Pres.*, 1992–1997, *Roswell*
Steve S. Torres, *Sec./Treas.*, 1991–1997, *Albuquerque*
Diane D. Denish, 1992–1997, *Albuquerque*
Delilah A. Vega, *Student Member*, 1995–1997, *Socorro*
Charles A. Zimmerly, 1991–1997, *Socorro*

New Mexico Institute of Mining and Technology
President . . . . . Daniel H. López

New Mexico Bureau of Mines and Mineral Resources
Director and State Geologist. . . . . Charles E. Chapin

Subscriptions: Issued quarterly, February, May, August, November; subscription price $10.00/calendar year.

Editorial Matter: Articles submitted for publication should be in the editor's hands a minimum of five (5) months before date of publication (February, May, August, or November) and should be no longer than 20 typewritten, double-spaced pages. All scientific papers will be reviewed by at least two people in the appropriate field of study. Address inquiries to Carol A. Hjellming, Editor of *New Mexico Geology*, New Mexico Bureau of Mines and Mineral Resources, Socorro, New Mexico 87801-4796.

Circulation: 1,000

Printer: University of New Mexico Printing Services

µm. Finally, at temperatures above 120 to 140°C, tracks that are formed are quickly destroyed and the fission-track age is zero. If, after a period of relative stability, the crust is rapidly cooled during denudation related to a tectonic event, the fossil PAZ may be exhumed and the time of cooling and the paleodepth of the top or bottom of the PAZ can be estimated (Gleadow and Fitzgerald, 1987). If the tectonically disturbed area cools rapidly (>5°C /m.y.), the mean track lengths in rocks that are at the base of the fossil PAZ (below the break-in-slope on the age-depth profile) are generally >14 µm, and the AFT ages from below the base of the exhumed PAZ can be used to estimate the timing of the onset of denudation. If the rock column cools more slowly during uplift and/or erosion, the mean track length at the base of the fossil PAZ is typically <14 µm, and the apparent AFT age more loosely constrains timing of the initiation of cooling (Foster and Gleadow, 1992).

Kelley et al. (1992) demonstrated that in areas undisturbed by late rift volcanism or hydrothermal activity, the timing of denudation of a rift flank (e.g., the Ladron Mountains north of Socorro) derived from AFT data closely fits the timing of denudation determined from the sediment record in the adjacent basin where early rift sediments have been uplifted and exposed. Similarly, in the present study, we will examine the cooling histories of the mountain ranges in the vicinity of the early rift basins described by Mack et al. (1994a, b) and compare our results with their provenance data. Because the denudation data from AFT analysis are consistent with the episodes of uplift and erosion preserved in areas where the sediment record is well studied, the technique can be used to determine the denudation history of uplifts adjacent to undissected basins where the sediment record is poorly understood.

Fission-track data collected in the northern Rio Grande rift of New Mexico and Colorado indicate that rocks now exposed in the eastern and western margins of the rift cooled during uplift, erosion, and waning volcanism in a complex, three-dimensional pattern (Kelley et al., 1992). Three interesting trends have emerged from the AFT data for the northern Rio Grande rift. First, the youngest AFT ages are found in the rift flanks adjacent to large normal faults along the deep margins of the en echelon half-grabens that make up the present Rio Grande rift. Second, promontories that project into rift basins at the junction of arcuate normal faults bounding the deep side of half grabens (Blanca Peak in the Sangre de Cristo Mountains and the Ladron Mountains) have some of the youngest AFT ages observed. Tectonic denudation on three sides has allowed unusually rapid isostatic uplift in these areas. Similarly, the Sangre de Cristo Mountains north of Blanca Peak are bounded on two sides by active late Cenozoic faults that have allowed the rapid isostatic rise of these mountains. Finally, cooling rates determined from the AFT age and length data have increased progressively from the Laramide orogenic event (1-4°C/Ma) to the development of the Rio Grande rift (7-20°C/Ma).

To see if these patterns are characteristic of the Rio Grande rift in general, samples for AFT analysis were collected from mountain ranges bordering and within the southern Rio Grande rift. The newly collected AFT age and length data will be used to constrain the cooling histories of portions of the eastern and western flanks and central horst blocks of the southern rift. The areas of study include the Caballo, Mud Springs, San Diego, Dona Ana mountains (central horsts); the Black Range (western flank); the San Andres, Organ, Franklin Mountains (central horsts); and Sierra Blanca, Capitan Mountains, Sacramento Mountains (eastern flank). These new data add to our understanding of vertical motions as a function of time and geographic location during compression and extension in the southern Rio Grande rift. In addition, the data can be used to compare and contrast the tectonic and topographic development of the northern and southern parts of the Rio Grande rift. Only two phases of extensional deformation are recognized in the northern rift north of Socorro whereas four phases have been documented in the south. The southern rift has undergone more extension compared to the north, as indicated by the wider zone of deformation and the thinner crust (Keller et al., 1990). Early rift magmatism is sparse to the north and more common to the south. Furthermore, rifting began about 7 to 8 Ma earlier in the southern rift (Mack et al., 1994a, b; Chapin and Cather, 1994).

The principal objectives of this paper are (1) to present new apatite fission-track ages for rocks exposed in the uplifts along the eastern and western margins and in the central horsts of the southern Rio Grande rift (Table 1, Fig. 1); (2) to use the AFT data to discuss the local tectonic and cooling history of each mountain block investigated; (3) to integrate the AFT data from all the mountain ranges and K-Ar data from intrusives in the southern rift into a discussion of the tectonic development of this region during Laramide compression, mid-Cenozoic volcanism, and Rio Grande rift formation; (4) to use the AFT results to compare and contrast the development of the northern and southern Rio Grande rift.

In addition, as an experiment, we attempted to more tightly constrain the age of the Eocene Love Ranch Formation in the Jornada del Muerto (LR, Fig. 1) by determining the AFT ages of granite clasts in the formation. The age of the Love Ranch Formation is currently thought to be between late Paleocene and middle Eocene, on the basis of radiometric ages of the overlying Rubio Peak Formation (40-43 Ma) and of the age of the youngest underlying unit (Seager and Clemons, 1975); few fossils have been found in the Love Ranch Formation (Seager et al., 1986). By assuming that the Proterozoic rocks from the Laramide Rio Grande uplift, which acted as the source region for the Love Ranch Formation, cooled during denudation and were transported immediately to the basin, we expect the clast AFT ages to provide some constraints on the timing of denudation in the Rio Grande uplift and to provide a maximum age for deposition of the Love Ranch Formation.

Fission-track analysis

Methods

The methods of fission-track analysis used in this study are fully described in Kelley et al. (1992). Thirty-one samples of Proterozoic igneous and metamorphic rocks, Paleozoic sedimentary rocks, and Eocene to Oligocene plutonic rocks were collected along reconnaissance traverses through ranges within and bordering the southern Rio Grande rift (Table 1, Fig. 1). In addition, 17 samples were collected in a more detailed study of the Eocene Organ batholith. The criteria used in locating the traverses included the occurrence of significant vertical relief and the presence of rock types containing adequate amounts of apatite for FT dating. Elevations of the samples were determined from U.S. Geological Survey 1:24,000-scale topographic maps to an estimated accuracy of ±6 m.

Apatite and zircon were separated from the samples using standard heavy liquid and magnetic separation techniques. Apatite grains were mounted in epoxy, polished to expose the grains, and etched for 25 seconds in a 5 M solution of nitric acid to reveal the fission tracks. The zircons were mounted in Teflon, polished, and etched in NaOH/KOH at 230°C for 4.5 hours (90SA01) and 8 hours (90BR05). The grain mounts were then covered with muscovite detectors and sent to the Texas A&M Nuclear Science Center for irradiation. The neutron flux was calibrated using the zeta technique with Durango apatite and Fish Canyon zircon age standards and Corning standard glasses CN-5 and CN-6. The zeta calibration is based on the accepted ages of 27.9 ±0.7 Ma for the Fish Canyon Tuff and 31.4 ±0.5 Ma for Durango apatite (Hurford and Green, 1983; Green, 1985).

The confined-track-length distributions in the apatite grain mounts were determined using a microscope fitted with a 100-X oil-immersion lens, a drawing tube, and a digitizing tablet. The system allows the track lengths to be measured to approximately ±0.2 µm. Horizontal, well-

TABLE 1—Apatite and zircon fission-track data for the southern Rio Grande rift, New Mexico.

Mountain range	Sample number	Rock type	Latitude longitude	Elevation (m)	Number of grains dated	ρ_s × 10^5 t/cm^2	ρ_i × 10^6 t/cm^2	ρ_d × 10^5 t/cm^2	Central age (Ma) (±1 S.E.)	P(χ)^2 (%)	Uranium content (ppm)	Mean track length (μm) (±1 S.E.)	Standard deviation track length
APATITE FISSION-TRACK DATA													
Caballo	90CAB01	Granite	33°04.98′ 107°14.24′	1482	20	0.34 (51)	4.94 (3659)	1.83 (3900)	**5.4 0.8**	99	36	N.D.	N.D.
	90CAB03	Granite	32°56.57′ 107°15.15′	1509	20	0.04 (5)	0.22 (121)	1.83 (3900)	**16.1 7.3**	60	2	N.D.	N.D.
	90CAB04	Granite	32°56.52′ 107°15.55′	1443	20	0.26 (40)	1.9 (1443)	1.83 (3900)	**10.8 1.8**	99	15	N.D.	N.D.
Mud Springs	90MS01	Meta-sediment	33°09.03′ 107°18.61′	1479	18	0.05 (5)	0.49 (230)	1.83 (3900)	**8.4 3.8**	99	4	N.D.	N.D.
San Diego	90SD01	Granite	32°35.74′ 106°58.95′	1395	20	0.08 (9)	1.55 (824)	2.8 (3756)	**6.5 2.2**	99	7	N.D.	N.D.
Doña Ana	90DA01	Dacite dike	32°28.29′ 106°46.47′	1440	20	0.15 (18)	0.66 (385)	1.83 (3900)	**18.2 4.4**	70	5	N.D.	N.D.
Black Range	90BR01	Copper Flat porphyry	32°56.22′ 107°31.69′	1677	20	0.42 (41)	1.5 (733)	1.83 (3900)	**21.7 3.6**	99	12	13.9 ± 0.4 (45)	1.3
	90BR03	Dacite	32°53.78′ 107°44.64′	2222	20	1.22 (98)	4.91 (1964)	1.83 (3900)	**19.4 2.2**	97	36	N.D.	N.D.
	90BR04	Dacite	32°54.34′ 107°42.67′	2006	20	0.28 (22)	0.9 (359)	2.8 (3756)	**36.6 8.1**	99	4	N.D.	N.D.
	90BR05	Dacite	32°51.08′ 107°31.89′	1594	20	1.79 (272)	3.34 (2541)	2.8 (3756)	**63.7 4.5**	99	16	14.3 ± 0.5 (52)	1.8
San Andres	90SA04	Granite	33°16.61′ 106°32.70′	1738	20	0.34 (35)	2.15 (1095)	3.08 (3756)	**21.0 3.7**	99	9	N.D.	N.D.
	90SA06	Gneiss	33°21.73′ 106°25.18′	1418	20	0.47 (29)	2.69 (828)	2.95 (3756)	**22.0 4.2**	99	12	N.D.	N.D.
	90SA08	Granite	32°51.02′ 106°34.40′	1456	20	0.31 (25)	1.8 (720)	2.95 (3756)	**21.8 4.5**	99	9	N.D.	N.D.
	90SA09	Granite	32°51.02′ 106°34.08′	1433	20	0.48 (48)	2.41 (1206)	2.95 (3756)	**25.0 3.8**	90	12	13.9 ± 1.0 (9)	1.5
	90SA10	Gneiss	32°51.16′ 106°33.20′	1387	20	0.12 (9)	2.04 (776)	2.8 (3756)	**6.9 2.3**	80	10	N.D.	N.D.
	90SA11	Amphibolite	32°51.36′ 106°32.68′	1433	20	0.16 (9)	1.22 (342)	2.8 (3756)	**15.7 5.3**	99	6	N.D.	N.D.
	90SA13	Granite	32°34.98′ 106°29.66′	1395	20	0.24 (10)	3.76 (789)	2.8 (3756)	**7.6 2.4**	90	18	N.D.	N.D.
	90SA14	Granite	32°35.55′ 106°29.42′	1543	20	1.38 (144)	5.22 (2714)	1.83 (3900)	**20.6 1.9**	75	38	13.4 (0.6) 10	0.9
	90SA15	Granite	32°51.21′ 106°34.16′	1529	20	0.22 (26)	1.95 (1133)	1.83 (3900)	**8.9 2.0**	90	14	14.5 (0.7) 13	1.3
	90SA16	Granite	32°35.96′ 106°27.87′	1445	20	0.38 (42)	1.87 (1030)	1.83 (3900)	**15.6 2.5**	99	14	N.D.	N.D.
	90SA17	Granite	32°35.71′ 106°27.98′	1439	20	0.69 (108)	6.6 (5152)	1.83 (3900)	**8.1 0.8**	75	50	14.9 (0.4) 45	1.5
Organ	81OR01	Aplite	32°22.41′ 106°32.52′	1570	9	1.91 (42)	5.92 (651)	1.21 (3027)	**16.6 2.7**	96	66	N.D.	N.D.
	81OR05	Quartz monzonite	32°21.10′ 106°33.13′	1844	20	1.14 (75)	3.73 (1232)	1.24 (3027)	**16.2 2.0**	99	39	14.3 ± 0.5 (53)	1.7
	81OR07	Quartz monzonite	32°21.83′ 106°33.46′	1890	17	0.96 (67)	4.93 (1727)	1.25 (3027)	**10.3 1.4**	98	54	13.9 ± 0.5 (100)	2.4
	81OR08	Quartz monzonite	32°25.5′ 106°34.0′	1744	18	1.61 (113)	6.34 (2219)	1.26 (3027)	**13.7 1.4**	99	66	14.3 ± 0.5 (100)	2.4
	81OR10	Quartz monzonite	32°23.35′ 106°35.75′	1662	20	0.57 (40)	1.44 (503)	1.27 (3027)	**21.4 3.6**	99	15	15.5 ± 1.1 (5)	1.4
	81OR12	Quartz monzonite	32°23.05′ 106°35.44′	1777	20	0.31 (25)	0.77 (311)	1.29 (3027)	**22.1 4.7**	99	9	N.D.	N.D.
	81OR13	Diorite porphyry	32°22.94′ 106°35.16′	1841	20	0.54 (29)	1.02 (275)	1.3 (3027)	**29.3 5.8**	99	12	13.6 ± 1.3 (24)	3.2
	81OR14	Quartz monzonite	32°23.00′ 106°35.00′	1872	20	0.56 (30)	1.8 (487)	1.31 (3027)	**17.2 3.3**	99	18	N.D.	N.D.
	81OR15	Quartz monzonite	32°22.92′ 106°34.79′	1951	20	0.12 (94)	0.5 (1917)	1.33 (3027)	**13.8 1.6**	99	51	14.2 ± 0.5 (90)	2.4
	81OR18	Rhyolite	32°22.46′ 106°34.67′	2165	20	0.4 (33)	1.2 (491)	1.35 (3027)	**19.3 3.6**	97	12	N.D.	N.D.
	81OR19	Rhyolite	32°23.49′ 106°34.59′	2293	17	0.25 (21)	0.57 (241)	1.37 (3027)	**25.2 5.8**	99	6	N.D.	N.D.

(continued on next page)

TABLE 1—Apatite and zircon fission-track data for the southern Rio Grande rift, New Mexico (*continued*).

Mountain range	Sample number	Rock type	Latitude longitude	Elevation (m)	Number of grains dated	ρ_s × 10^5 t/cm^2	ρ_i × 10^6 t/cm^2	ρ_d × 10^5 t/cm^2	Central age (Ma) (±1 S.E.)	P(χ)^2 (%)	Uranium content (ppm)	Mean track length (μm) (±s1 S.E.)	Standard deviation track length
APATITE FISSION-TRACK DATA (*continued*)													
	81OR20	Quartz monzonite	32°23.21′ 106°34.58′	2043	20	0.36 (29)	0.94 (374)	1.38 (3027)	**22.5 4.4**	99	9	11.6 ± 1.6 (24)	3.9
	81OR21	Quartz monzonite	32°21.1′ 106°30.8′	1768	20	1.71 (188)	6.83 (3755)	1.4 (3027)	**14.7 1.3**	92	66	14.6 ± 0.3 (100)	1.5
	81OR22	Quartz monzonite	32°21.45′ 106°31.75′	1616	20	0.78 (77)	3.5 (1713)	1.41 (3027)	**13.2 1.6**	99	33	14.8 ± 0.4 (34)	1.2
	81OR23	Quartz monzonite	32°26.17′ 106°33.18′	1655	10	1.16 (65)	4.55 (1274)	1.43 (3027)	**15.2 2.0**	80	45	N.D.	N.D.
	81OR24	Quartz monzonite	32°21.85′ 106°34.22′	2068	10	0.62 (30)	2.71 (651)	1.45 (3027)	**14.2 2.7**	85	24	N.D.	N.D.
	81OR25	Tuff	32°14.4′ 106°34.0′	?	20	1.24 (137)	5.04 (2771)	1.46 (3027)	**15.4 1.5**	99	45	13.8 ± 0.5 (93)	2.6
Franklin	90FR01	Thunderbird rhyolite	Transmoun-tain Road	?	20	0.12 (12)	0.18 (89)	1.8 (3825)	**51.8 15.8**	99	3	N.D.	N.D.
Sierra Blanca	90SB02	Syenite	33°27.53′ 105°37.30′	2265	20	1.58 (101)	5.15 (1648)	1.83 (3900)	**23.8 2.6**	99	39	14.4 ± 0.4 (88)	2
	90SB03	Syenite	33°23.52′ 105°46.78′	3070	20	0.33 (30)	0.98 (440)	1.83 (3900)	**26.5 5.1**	99	7	N.D.	N.D.
	90SB04	Syenite	33°24.54′ 105°45.29′	2780	20	0.42 (46)	1.01 (544)	1.83 (3900)	**32.8 5.2**	99	7	15.7 ± 0.5 (9)	0.8
Capitan	CAPT35	Granite	33°33.59′ 105°12.74′	1900	20	1.03 (49)	2.52 (602)	1.61 (3625)	**27.9 4.3**	99	21	N.D.	N.D.
Sacra-mento	90SAC04	Abo Sandstone	32°56.46′ 105°50.46′	2058	20	0.18 (23)	0.19 (121)	2.8 (3756)	**112.7 25.3**	99	3	11.4 ± 1.6 (12)	2.8
	91SAC05	Trachyte	32°41.21′ 105°52.60′	1317	20	0.48 (24)	0.84 (2111)	1.67 (3825)	**40.7 8.8**	99	7	N.D.	N.D.
	91SAC06	Trachyte	32°41.21′ 105°52.60′	1317	20	0.29 (20)	0.59 (202)	1.67 (3825)	**35.4 8.3**	99	5	N.D.	N.D.
	91BENT5	Diorite	33°09.40′ 105°50.60′	1829	20	0.92 (46)	1.27 (318)	1.67 (3825)	**51.7 8.2**	99	10	N.D.	N.D.
	91BENT9	Diorite	33°09.40′ 105°50.60′	1829	20	1.15 (55)	1.22 (293)	1.67 (3825)	**67.0 10.0**	70	10	10.1 ± 1.4 (13)	2.6
	CL ASH	Tuff (?)	32°57.62′ 105°44.57′	2646	16	0.22 (21)	1.45 (137)	1.52 (3785)	**49.3 11.7**	97	3	N.D.	N.D.
Jornada del Muerto Basin	93LR01	Granite clasts	32° 57.94′ 107°00.33′	1411	15	1.68 (69)	6.83 (1407)	1.34 (3525)	**14.0 1.0**	99	68.4	14.0 ± 0.7 (22)	1.8
	93LR02	Granite clasts	32° 57.94′ 107°00.33′	1411	20	2.64 (195)	6.67 (2466)	1.34 (3525)	**22.7 0.9**	99	66.6	14.3 ± 0.5 (33)	1.4
	93LR03	Granite clasts	32° 57.94′ 107°00.33′	1411	20	0.16 (20)	0.68 (434)	1.34 (3525)	**13.2 3.1**	99	6.8	N.D.	N.D.
ZIRCON FISSION-TRACK DATA													
Black Range	90BR05	Dacite	32°51.08′ 107°31.89′	1594	6	25.96 (351)	5.68 (384)	3.29 (4009)	**68.0 5.4**	99	220	N.D.	N.D.
San Andres	90SA01	Rhyolite	33° 17.82′ 106°33.55′	1974	6	39.82 (446)	10.52 (589)	2.91 (4009)	**49.6 3.8**	99	450	N.D.	N.D.

ρ_s - spontaneous track density

ρ_i - induced track density (reported induced track density is twice the measured density)

ρ_d - track density in muscovite detector covering CN-6 (1.05 ppm) or CN-5 (10 ppm). Reported value determined from interpolation of values for detectors covering standards at the top and bottom of the reactor packages (fluence gradient correction).

Number in parenthesis is the number of tracks counted for ages and fluence calibration or the number of tracks measured for lengths.

S.E. = standard error

P(χ)^2 = Chi-squared probability

N.D. = no data

$\lambda_f = 1.551 \times 10^{-10} yr^{-1}$, g = 0.5

zeta = 4265 ± 300 for apatite, 452 ± 56 for zircon

Mean track lengths not corrected for length bias (Laslett et al., 1982)

etched, confined tracks (tracks completely enclosed within the crystal) in grains with prismatic faces were measured. The orientation of the tracks with respect to the c-axis was also measured. Time-temperature estimates were derived from the age and track-length data using the inverse-modeling algorithm of Corrigan (1991). The values of *A*, *Q*, and *n* used in this investigation are the composite parameters of Carlson (1990), and an initial track length of 15.7 μm is assumed for the models.

Results

The interpretation of the AFT data for each traverse (Fig. 1) is considered in detail in the following sections. First, we will examine the AFT data from the Caballo, Mud Springs, San Diego, and Dona Ana Mountains and compare the results with the interpretations of Mack et al. (1994a, b). We will then discuss the AFT data from areas where the Cenozoic uplift and sedimentation history are not as well documented. The cooling rates estimated from the AFT results are in Table 2. Unfortunately, because the uranium content of many of the apatites from the southern rift is low (<5 ppm), detailed track length analysis and thermal modeling was possible for only nine of the samples.

Caballo, Mud Springs, San Diego, Doña Ana mountains—The Caballo Mountains are an east-dipping fault block with Proterozoic granitic and metasedimentary rocks exposed on the western side (Fig. 2). Paleozoic to Mesozoic sedimentary rocks overlie the Proterozoic rocks and form the eastern dip slope into the Jornada del Muerto. The Paleozoic sedimentary rocks that form the crest of the range are dominated by carbonates lacking apatite, so an age-elevation traverse through the range was not possible. A northwest- to north–northwest-trending Laramide basement-cored uplift is preserved in the Caballo Mountains; this uplift, which is related to the Rio Grande uplift (Seager and Mack, 1986), shed sediments northward into a broad Laramide basin preserved as the Love Ranch Formation in the modern Jornada del Muerto. The southern end of the Caballo Mountains once floored one of the early, broad rift basins (Seager et al., 1984). The cooling history recorded by AFT dates from the Proterozoic rocks at low elevation on the west side of the range is dominated by denudation during the later phases of rift development. The AFT ages are 5.4 ±0.8 Ma on the northern end and 10.8 ±1.8 to 16.1 ±7.3 Ma in the south-central part of the range.

Mack et al. (1994a, b) noted that early unroofing of the Caballo Mountains is recorded in the Hayner Ranch Formation (approximately 25 to 16 Ma). The lower part of this formation contains clasts from the youngest part of the stratigraphic

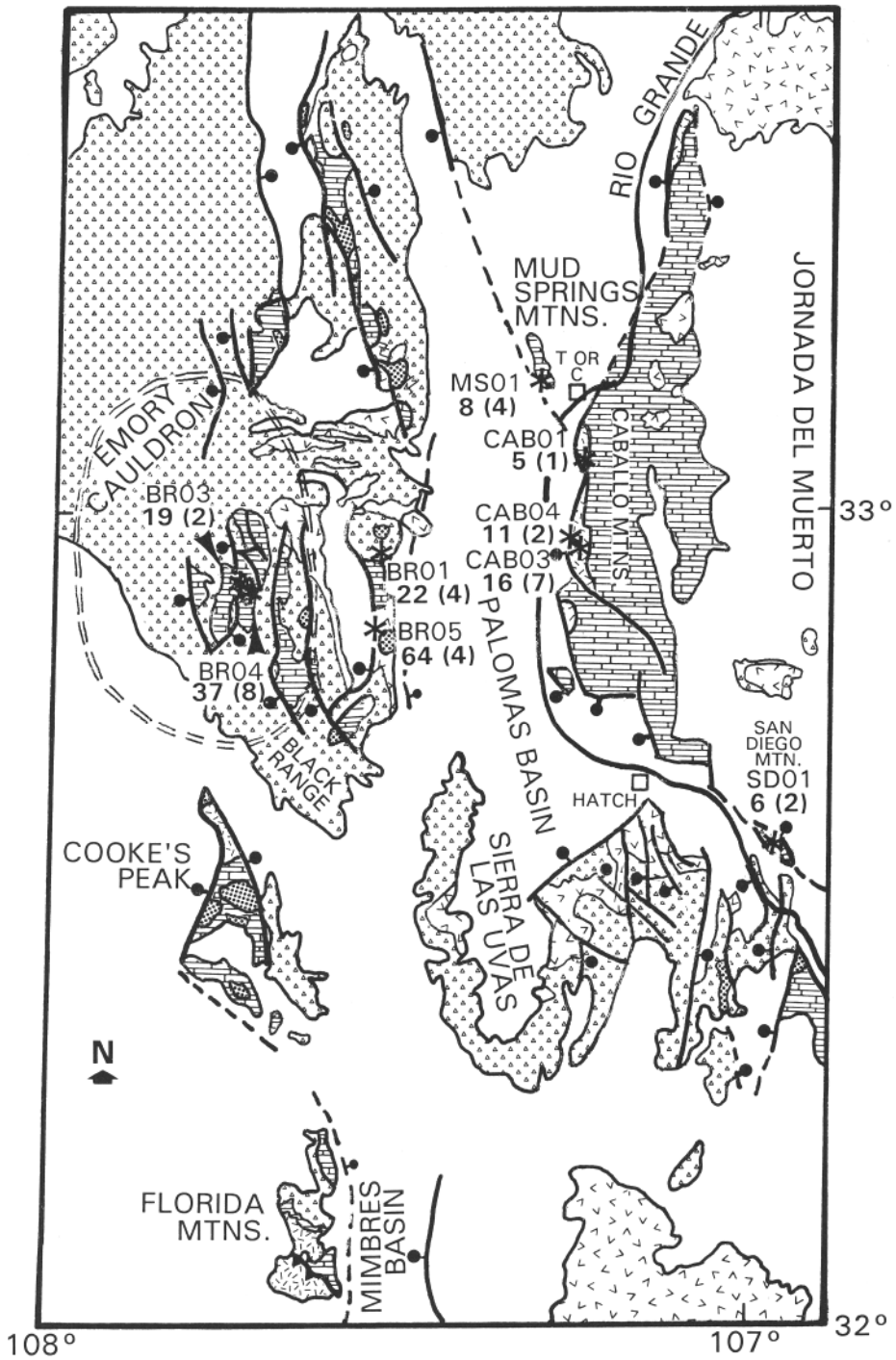

FIGURE 2—Simplified geologic map after Woodward et al. (1978) generally corresponding to the western half of Fig. 1. Sample localities shown as asterisks labeled with the sample numbers and ages; the standard error of the ages is enclosed in parentheses. See Table 1 for data and Fig. 3 for explanation of units.

TABLE 2—Cooling rates derived from track-length analysis using the model of Corrigan (1991).

Sample number	Age range (Ma)	Temperature range (°C)	Cooling rate (°C/Ma)
90BR01	17–11	120–60	10
	11–5	60–50	2
90BR05	65–0	120–10	2
81OR05	22–10	120–40	7
81OR07	11–0	120–10	10
81OR08	12.5–5	120–40	11
81OR15	13–6	120–35	12
81OR21	14–5	120–25	10
81OR25	14–6	120–50	9
90SB02	21–10	120–45	7

section (Oligocene Uvas Basaltic Andesite and Bell Top tuff); the upper part of the formation consists of clasts derived from the Eocene Palm Park and Love Ranch Formations. The basal part of the overlying Rincon Valley Formation (about 16 to 6 Ma) is similar to the Hayner Ranch in that it includes Uvas, Bell Top, Palm Park, and Love Ranch clasts. In contrast, in the middle to upper beds of the Rincon Valley Formation, clasts of Permian Abo Formation and Pennsylvanian Magdalena Group limestones are abundant. No Proterozoic granite clasts are found in the Rincon Valley Formation, except for those thought to be reworked from the Eocene Love Ranch Formation. These observations are consistent with the AFT data. The average modern heat flow in the Palomas Basin on the west side of the mountains is about 95 mW/m^2, and the average gradient is on the order of 30 to 35°C /km (Reiter et al., 1986; Reiter and Barroll, 1990). Assuming that the average heat flow has not changed since extension began and assuming a surface temperature of 15°C, the base of the apatite PAZ (120°C) was at a depth of 3 to 3.5 km in the late Eocene. On the basis of the geologic cross-section *A-A'* of Seager et al. (1982), at least 3 km of Paleozoic to Middle Cenozoic sedimentary and volcanic rocks may have overlain the Proterozoic rocks prior to denudation of the Caballo Mountains. The AFT ages from low-elevation Proterozoic rocks in the south-central Caballo Mountains record cooling through the PAZ for apatite during deposition of the Rincon Valley Formation at the time the Proterozoic rocks were still in the subsurface. These Proterozoic rocks were exposed at the surface later; Proterozoic detritus is common in the early Pliocene to middle Pleistocene Palomas Formation (Lozinsky and Hawley, 1986; Mack and Seager, 1990) in the Palomas Basin to the west. The decrease in AFT age to the north and depositional trends of Proterozoic detritus imply that the fault that was active during late Oligocene to Miocene time along the southeastern margin of the Caballo Mountains propagated northward during latest Miocene to Pliocene time (G. Mack, written comm. 1996).

The Mud Springs Mountains (Fig. 2) are a small, east-dipping intrarift horst block with a small outcrop of Proterozoic metasedimentary rocks exposed along the southwest side; the metamorphic rocks are overlain by Paleozoic sedimentary rocks. As in the case of the northern Caballo Mountains, the AFT age of 8.4 ±3.8 Ma for the Proterozoic rocks records rapid cooling during the later phases of rifting.

San Diego Mountain (Fig. 2) is another small intrarift horst block. The northern marginal thrust fault of the Laramide Rio Grande uplift, which brought Proterozoic rocks near the surface, is exposed along the north side of the mountain (Seager,1986). The area subsequently formed part of the early rift basin preserved in the southern Caballo Mountains. The early rift basin was then broken up during the later phases of rift development. The AFT age of 6.5 ±2.2 Ma on Proterozoic granite appears to be the result of cooling during the latest episode of normal faulting in the late Miocene. Late Quaternary uplift of this block is recorded by a 30-m offset in the Camp Rice Formation (Seager, 1986). Seager (1986) proposed that the highly silicified outcrop of Camp Rice Formation that rests on the Proterozoic granite represents a fossil hot-spring deposit. Anomalously high modern heat flow in a shallow-flow system northwest of San Diego Mountain was observed by Reiter et al. (1978). The water in the fossil hydrothermal system apparently was not hot enough, or the system was so short lived, that it did not completely reset the AFT ages to ages younger than the Quaternary Camp Rice Formation.

One sample from a dacite dike on the east side of the Dona Ana Mountains (Fig. 3), which may be part of a small cauldron within the Organ cauldron (Seager and McCurry, 1988), was collected to investigate the cooling history of this range. An AFT age of 18.4 ±4.4 Ma was determined. Mack et al. (1994a, b) see evidence for uplift of the Dona Ana Mountains beginning with the deposition of the Rincon Valley Formation. Pennsylvanian Panther Seep Formation and Tertiary rhyolite clasts that are unique to the Doña Ana Mountains are found in the Rincon Valley Formation but not in the underlying Hayner Ranch Formation. Because the AFT and provenance results from the southern Caballo area are compatible, we will now apply this technique to areas in the southern rift where the Oligocene to Miocene uplift and sedimentation history are concealed by younger basin fill.

Black Range-The remnants of the Emory cauldron, which is part of the large Mogollon-Datil volcanic field, are exposed in the Black Range on the west side of the Palomas Basin (Fig. 2). Volcanism began in the area about 38 Ma and the cauldron formed with the eruption of the voluminous 35.2 Ma Kneeling Nun Tuff (Elston, 1989; McIntosh et al., 1992a). The caldera floor was subsequently domed upward by resurgence, and the moat between the caldera wall and dome was largely filled with younger lava and pyroclastic flows from local and distant sources (Elston, 1989). Tuffs preserved in the Black Range are 35.2 to 28.1 Ma (McIntosh et al., 1992a). Most of the faults related to cauldron collapse have been reactivated during rift-related deformation.

A Proterozoic granitic outcrop north of Kingston was sampled as part of this study, but this particular granite contains fluorite, not apatite so no AFT data are available. The two highest-elevation samples are from Tertiary andesitic intrusives southeast of Kingston. Maggiore (1981) determined a zircon FT age of 34.0 ±2.8 Ma for the andesite porphyry sill at the location of 90BR04 (Table 1). The AFT age of 36.6 ±8.1 Ma is concordant with the zircon FT age and is indicative of rapid cooling of this shallowly emplaced sill. In contrast, the dacite intrusive exposed at slightly higher elevation (90BR03) is significantly younger (19.4 ±2.2 Ma) than 90BR04. The eastern margin of the Emory cauldron, which is located adjacent to this sample, has been reactivated a number of times following the collapse of the cauldron (Abitz, 1986), complicating the cooling history of this area.

The two lower-elevation samples are from a small horst block east of Hillsboro. One sample (90BR01, Table 1), with an AFT age of 21.7 ±3.6 Ma, is from the 73.4 ±2.5 Ma (K-Ar age; Hedlund, 1974) Copper Flat stock. The long mean track-length measurements for this sample indicate rapid cooling. The other sample (90BR05), which is from a small outcrop labeled Tii on the map of Seager et al. (1982), surprisingly yielded Cretaceous apatite and zircon FT ages (Table 1). Because the zircon FT age of 68.0 ±5.4 Ma is nearly concordant with the AFT age of 63.7 ±4.5 Ma and the mean track lengths are long (Table 1), the intrusive cooled rapidly (>40°C /Ma) from the blocking temperature of 240 ±50°C (Hurford, 1986) for fission tracks in zircon to approximately 120°C during the Late Cretaceous. Since about 65 Ma, the cooling rate slowed to 2°C /Ma. This outcrop has not been significantly heated since the Cretaceous.

Despite the complex structures and age patterns in this area, the AFT data provide some constraints on the cooling history of the Black Range. Much of the thermal history of this area is related to cooling following mid-Cenozoic igneous activity in this region. The discovery of a previously unknown Cretaceous intrusion yielding a 64 Ma AFT age suggests that post-Cretaceous burial of the horst block southeast of Hillsboro was not great enough to reset the AFT age, which is congruous with the thin (<1 km) Cenozoic volcanic and sedimentary section preserved in this area (G. Mack, written comm. 1996). However, the Copper Flat stock to the north remained in the subsurface and began to cool in the early Miocene. These observations are corroborated by the distribution of volcanic clasts in the Late Cretaceous to early Tertiary McRae Formation exposed in the northeastern Caballo Mountains. Clasts that are chemically identical to the porphyry in the recently discovered Cretaceous intrusion have been found in this unit, but clasts from the Copper Flat stock have not been detected in the McRae Formation (N. McMillan, written comm. 1995).

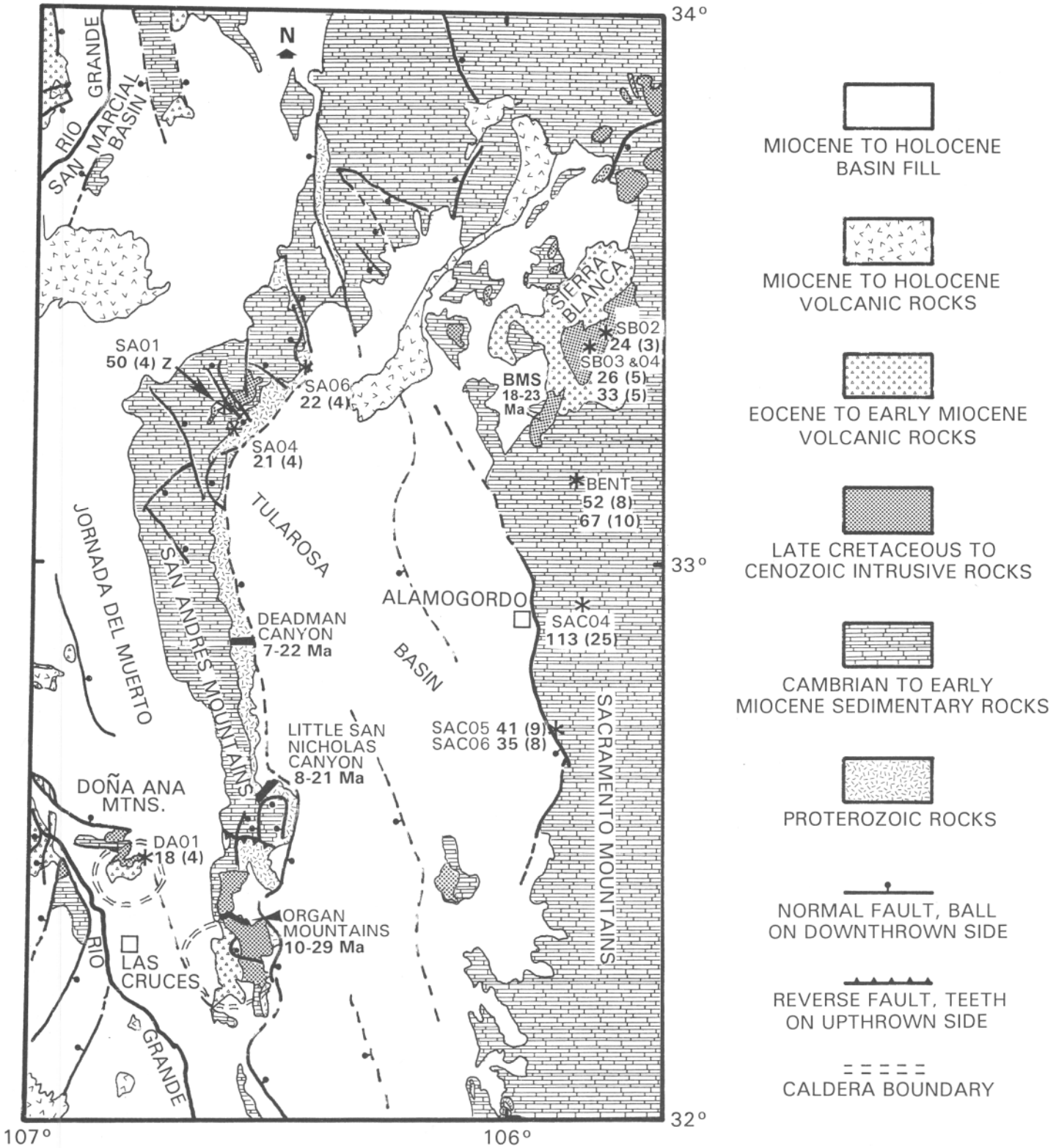

FIGURE 3—Simplified geologic map generally corresponding to the eastern half of Fig. 1 (after Woodward et al., 1978). Sample localities shown as asterisks labeled with the sample numbers and ages; the standard error of the ages is enclosed in parentheses. Sample traverses in the San Andres and Organ Mountains are represented by bold lines, and the range of AFT ages along the traverses is shown on the map. **BMS**, Black Mountain Stock. See Table 1 for data.

San Andres Mountains—The San Andres Mountains (Figs. 1, 3) are a west-tilted fault block, with Paleozoic sedimentary rocks (primarily carbonates) restingon Proterozoic igneous and metamorphic rocks. Virtually nothing has been published on the Cenozoic uplift history of the San Andres Mountains for two reasons. First, the range is bounded on both sides by undissected basins, the Jornada del Muerto on the west and the Tularosa Basin on the east. Second, the San Andres Moun-

Mountains are within White Sands Missile Range, so access is restricted. AFT samples were collected from three traverses through the Proterozoic rocks exposed on the east side of the San Andres Mountains. In addition, samples were collected from the undated rhyolite sill exposed on Salinas Peak near the north end of the range. The zircon FT age of the rhyolite sill is 49.6 ±3.8 Ma (90SA01, Table 1); no apatite was recovered from the rhyolite.

The AFT ages of approximately 21 to 22 Ma (Table 1; Fig. 3) were determined from Proterozoic rocks at the north end of the range. A traverse through Dead Man Canyon (Fig. 3) in the central part of the range yielded AFT ages of 7 to 22 Ma. The approximately 22 Ma ages are generally found in the stratigraphically highest part of the Proterozoic section a short distance below the Cambrian Bliss Sandstone and the 15 to 7 Ma ages are from stratigraphically lower levels. An exception to this generalization is 90SA15 (8.9 ±2 Ma), which is located on the upthrown side of a west-dipping normal fault that offsets Paleozoic and Proterozoic rocks in this area (Seager et al., 1982). The southern traverse is in the structurally complicated Little San Nicolas Canyon area (Fig. 3; Roths, 1991). Again, the ages in this canyon are between 8 and 21 Ma, but in this case, the youngest ages strictly coincide with north-trending, high-angle faults cutting the Proterozoic granites and gneiss. Roths (1991) mapped these faults as thrust faults, but the AFT data imply that these faults have been reactivated during extension, with the youngest ages exposed on the upthrown block. One possible interpretation of this limited AFT data set is that the San Andres Mountains started cooling during an early phase of extension and that a later phase of rapid cooling is recorded in samples near high-angle faults in the Dead Man Canyon and San Nicolas Canyon areas (Table 2).

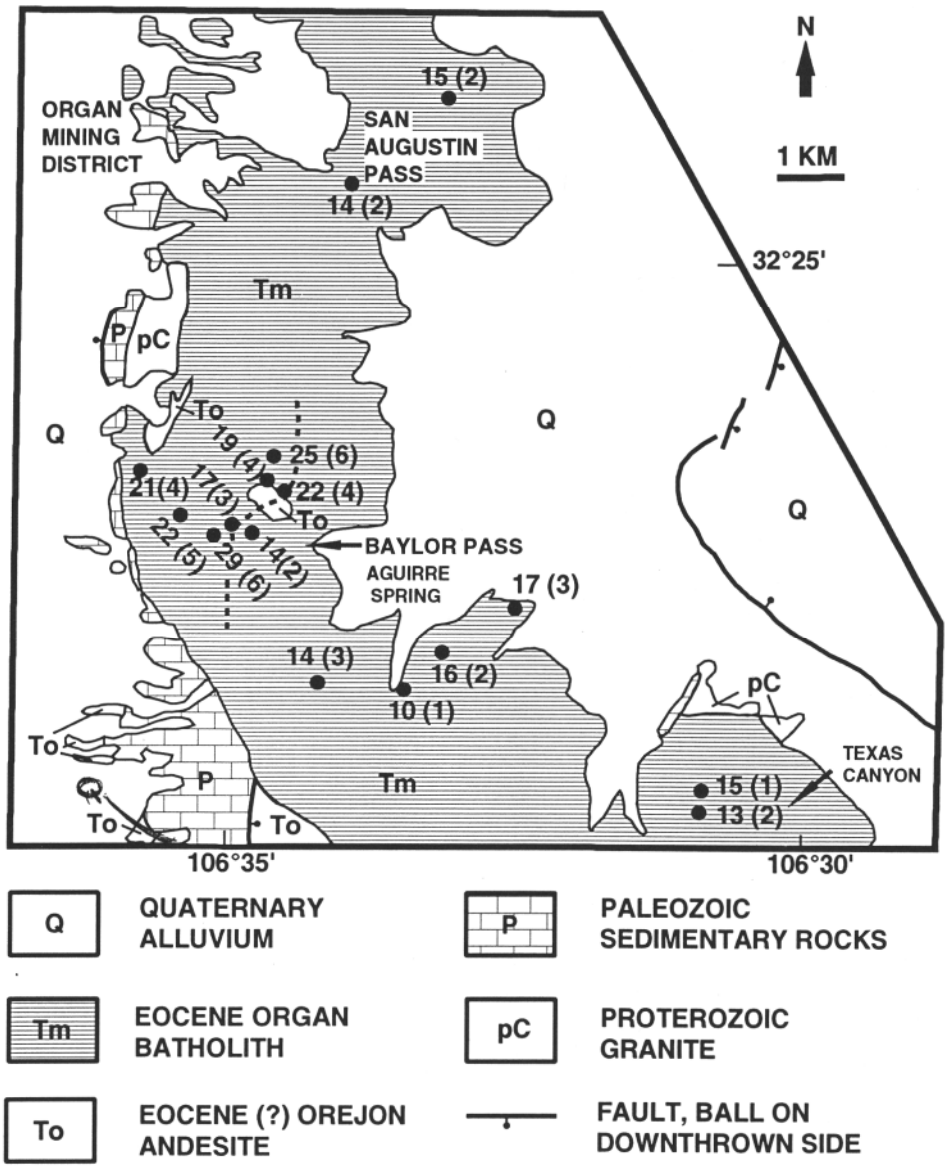

FIGURE 4—Simplified geologic map of the Organ Mountains (after Seager, 1981). The AFT ages and standard error (in parenthesis) are shown. The sinuous line in the center of the range marks the approximate boundary between the uplifted, rotated zone of protracted cooling (PAZ) to the west from rocks that were more rapidly cooled to the east.

Organ Mountains—The Organ Mountains (Fig. 3) are, in large part, the erosional remnant of the late Eocene Organ cauldron. The Organ batholith intrudes Proterozoic rocks, Paleozoic sedimentary rocks, and the Eocene Orejon Andesite, as well as the pyroclastic flows and lavas associated with the formation of the cauldron (Seager, 1981). The Organ batholith consists of four plutonic phases, two hypabyssal phases, and a variety of silicic dikes (Seager, 1981). The silicic magma that formed the Organ batholith was emplaced at shallow depths, and the upper part of this magma body erupted to produce three large ash-flow tuff units. Approximately 3 km of tuffs were deposited and preserved in the subsiding cauldron. These tuffs were erupted between 35.7 to 36.2 Ma, on the basis of $^{40}Ar/^{39}Ar$ ages and paleomagnetic data of McIntosh et al. (1992a). The cauldron likely developed in an extensional setting because normal faults that offset the tuffs are intruded by batholithic rocks (Seager and McCurry, 1988). The final phase of volcanism in the area is represented by 300 m of rhyolitic to trachytic lavas. Subsequently, the area has been block faulted and rotated about 15-20°W. Most of the mineralization in the Organ Mountains is related to emplacement of the batholith (Seager, 1981), but mineralized veins and dikes that cut the Sugarloaf Peak quartz monzonite in the northern part of the batholith may have formed after these rocks crystallized. The dikes and quartz monzonite have been intensely sericitized in the Organ mining district in the northeastern part of the batholith (Fig. 4).

The AFT ages from the Organ batholith range from about 10 to 29 Ma. The ages do not show a significant increase with increased elevation, but the ages on the west side are generally older than those on the east side (Figs. 4, 5), a trend that is consistent with the westward dip of the batholith. The age-elevation data and the track-length data for the east-side samples (81OR05, 06, 08, 21, 22) indicate a relatively simple, rapid (7-11°C / Ma; Table 2, Fig. 5) cooling history for this part of the batholith. Sample 81OR15 at Baylor Pass is significantly younger than the adjacent samples. The track-length data for 81OR15 indicate that it cooled rapidly (12°C /Ma; Table 2). Track-length data for nearby samples 81OR13 (13.6 ±1.3, n=24) and 81OR20 (11.8 ±1.6, n=24; Fig. 5) suggest that the west-side samples experienced protracted cooling during the late Oligocene prior to rapid tilting and denudation of the batholith 14 to 17 Ma. The sinuous

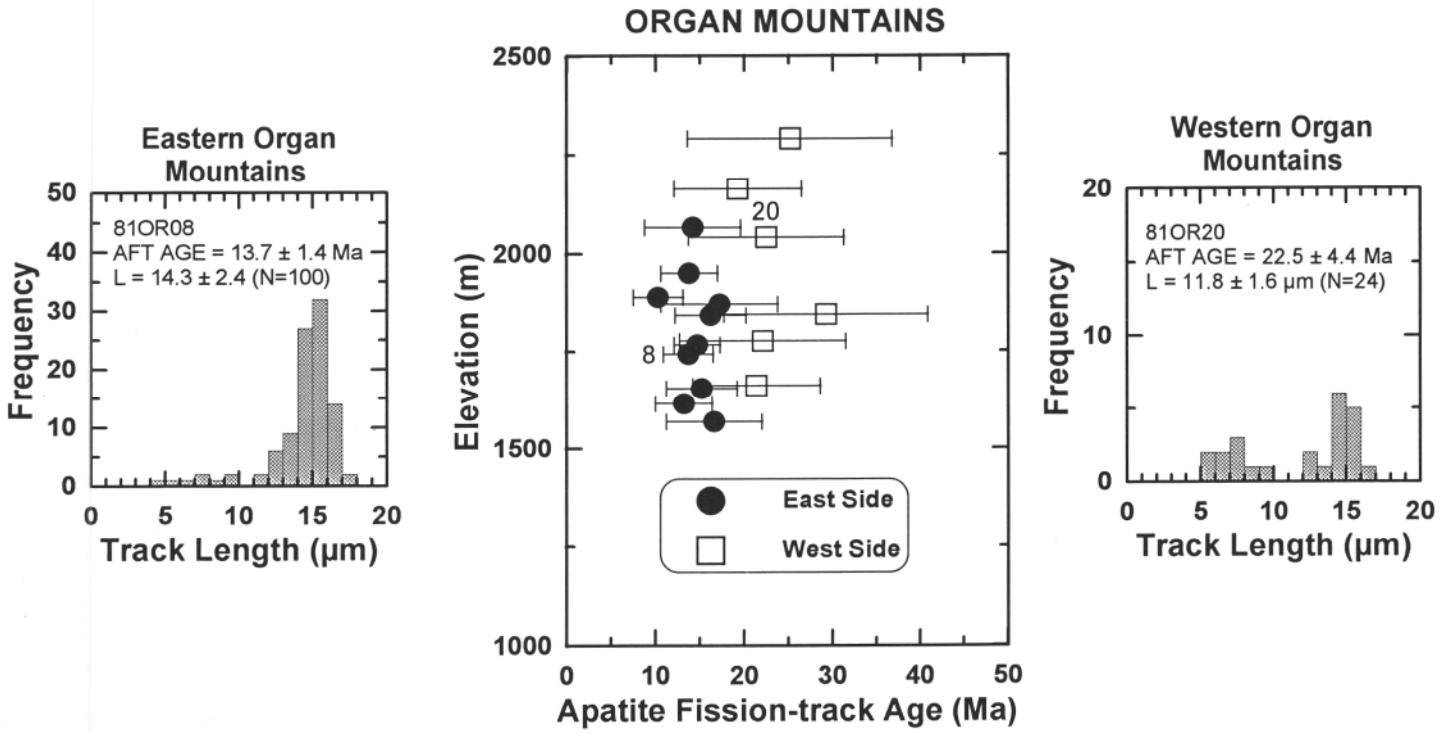

FIGURE 5—Age-elevation plot for the eastern (solid circles) and western (open squares) Organ Mountains with 2 σ error bars. Representative track-length histograms for the eastern and western Organ Mountains are shown with sample number, age and standard error of the age, mean track length, standard deviation of length, and number of length measurements (in parentheses).

line on Fig. 4 marks the approximate boundary between the uplifted, rotated zone of protracted cooling (PAZ) on the west side from rocks that were more rapidly cooled on the east side.

Franklin Mountains-Pam Roths (oral comm. 1991) provided a sample of Proterozoic Thunderbird rhyolite from high elevation on the Franklin Mountains, a west-tilted fault block south of the Organ Mountains (Fig. 1). The AFT age for this low-uranium apatite is 51.8 ±15.8 Ma. This relatively old AFT age from high elevation suggests the possibility that an uplifted PAZ may be present in the Franklin Mountains. An age-elevation traverse is needed to investigate this possibility.

Sierra Blanca, Capitan, Sacramento mountains-Sierra Blanca (Figs. 1, 3), which lies north of the Sacramento Mountains, forms part of the eastern margin of the rift and is the highest mountain in the southern rift (3,658 m). Sierra Blanca consists primarily of Eocene (38 Ma) andesitic volcanic rocks overlying Cretaceous to Paleocene sedimentary rocks. Four Oligocene-Eocene (25-38 Ma) syenite-monzonite-granite stocks intrude the sedimentary and volcanic rocks (Thompson, 1972; Moore et al., 1991). The AFT data from the stocks can be used to examine the post-Oligocene cooling history of this part of the eastern flank of the rift. Apatite ages for the syenite porphyry part of the Three Rivers stock at high elevation are 26.5 ±5.1 and 32.8 ±5.2 Ma (905B03 and 905B04; Fig. 3). These AFT ages are nearly concordant with the 29.9 ±1.8 Ma K-Ar age on amphibole determined by Moore et al. (1991), indicating rapid cooling of this intrusion at shallow levels in the crust. Similarly, an AFT age of 23.8 ±2.6 Ma and high-mean-track length of 14.4 ±0.4 μm (Table 1) for the Bonito Lake stock (26.6 ±1.4 Ma K-Ar on biotite; Moore et al., 1991) suggest rapid cooling of this intrusion (90SB02; Fig. 3).

In contrast to the high-elevation samples with their rapid, simple cooling histories, the lower-elevation samples had a more protracted, and perhaps complicated, cooling history following emplacement. The AFT dates of 17.5 and 22.6 Ma reported by Allen and Foord (1991) for Black Mountain stock (BMS, Fig. 3) are significantly younger than the 37.8 and 34.6 Ma $^{40}Ar/^{39}Ar$ ages on hornblende and plagioclase, respectively, for this intrusion and its associated dikes. No track-length data were presented for these samples. An attempt was made to determine the AFT age of a syenite porphyry dike near Three Rivers campground along the western base of Sierra Blanca, but the apatite contains abundant defects that obscured the fission tracks.

The 28.3 ±0.1 Ma Capitan pluton (Campbell et al., 1994) lies northeast of Sierra Blanca (Fig. 1). This large granitic batholith is oriented east-west and parallels the Capitan lineament (Chapin et al., 1978a). Fluid-inclusion data indicates that the Capitan pluton, the top of which now stands about 1 km above the surrounding plains, was intruded beneath at least 1 km of rock (Allen and McLemore, 1991; Campbell et al., 1994). An AFT age from low elevation on the eastern margin of the pluton is 27.9 ±4.3 Ma. Because the AFT age is concordant with the $^{40}Ar/^{39}Ar$ age on feldspar, this shallowly emplaced pluton cooled rapidly.

The Sacramento Mountains (Figs. 1, 3), an east-tilted fault block that marks the transition from the southeastern Rio Grande rift to the Great Plains, are dominated by Paleozoic carbonates, so the opportunity for collection of samples with abundant apatite and zircon is somewhat limited. Attempts to recover apatite from sandstone lenses in the Ordovician, Pennsylvanian, and Permian carbonate sections exposed on the west side of the range were unsuccessful. Apatite was found in Proterozoic metasedimentary rocks south of Alamogordo at the base of the west-facing Sacramento escarpment, in the Permian Abo Formation near High Rolls, and in Proterozoic intrusive rocks in the Bent dome. Although there is insufficient material for a complete traverse through the range, the datable samples do provide some information on the Cenozoic cooling history of this mountain block.

The highest-elevation sample, 90SAC04 (Table 1, Fig. 3), which is from the Permian Abo Formation, has an AFT age of 112.7 ±25.3 Ma. On the basis of limited track-length data (11.4 ±2.8 μm; n=12), this rock unit likely resided in the PAZ for a sub-

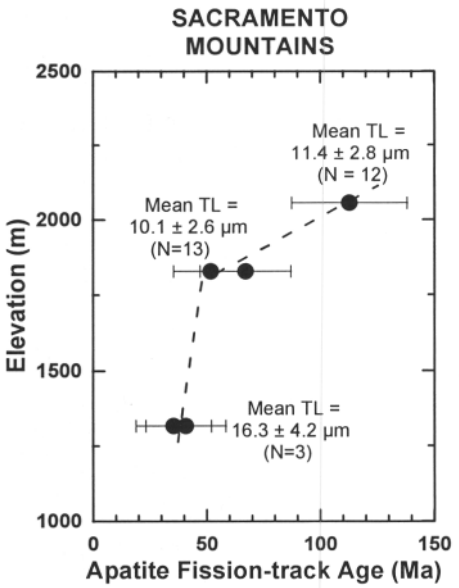

FIGURE 6—Age-elevation plot with 2σ error bars for the Sacramento Mountains. The break in slope of the dashed line shows the approximate position of the base of the uplifted PAZ.

stantial period of time prior to denudation. The Proterozoic rocks in the Bent area to the north have AFT ages that are in the 52 to 67 Ma range, and the mean track lengths are also short (10.1 ±2.6 µm; n=13). Like the Abo samples, these age and length data are characteristic of samples found in a PAZ that likely formed at a time of relative tectonic stability during Mesozoic burial of the area (Fig. 6). Bowsher (1991) proposed, on the basis of facies distribution patterns near Sierra Blanca, that uplift in the Sacramento Mountains may have started in the early Mesozoic; however, the AFT age and length data indicate that little denudation was associated with this minor disturbance. The 35 to 41 Ma AFT ages and the mean track length of 16.3 ±4.2 µm (n=3) from the base of the western Sacramento escarpment can be used to infer that the Mesozoic PAZ was brought toward the surface by uplift and erosion during the earliest phase of extension and was brought to the surface by the latest phase of rifting. The preservation of old ages at high elevation (Fig. 6) indicate that this mountain range was not strongly uplifted early in the development of the rift. Further work on the Permian red beds in this area is needed to test this interpretation.

An interesting deposit that appears to be an intensely altered volcanic ash was discovered in a sinkhole in the Permian Yeso Formation on the outskirts of Cloud-croft in the Sacramento Mountains. Although this fine-grained deposit contains no identifiable glass shards or zircon, it does contain subhedral grains of apatite with an AFT age of 49.3 ±11.7 Ma (CL ash, Table 1). This age is similar to the K-Ar age of the oldest intrusive in the Orogrande area (Table 3) and to the age of dikes and sills in the Sacramento Mountain escarpment west of Cloudcroft (45.3 ±2.2 Ma, Asquith, 1974; Fig. 1).

TABLE 3—Published and unpublished K-Ar ages of early to middle Eocene intrusive rocks from the southern Rio Grande rift. Date for Cuchillo Mountain stock is from Chapin et al. (1978b). **h**, hornblende; **b**, biotite.

Intrusive name	Phase dated	Latitude longitude	Age (Ma)
Cuchillo Mtn. stock	h	33°20.00′ 107°34.00′	50.1±2.6
Orogrande syenodiorite (oldest intrusive)	b	32°28.92′ 106°06.92′	48.3±1.8
Orogrande quartz latite	h	32°24.25′ 106°06.25′	42.6±2.2
Tres Hemanos stock	h	31°53.83′ 107°42.48′	50.3±2.6

Discussion

The reconnaissance nature of this study and the lack of datable rocks at high elevations in several of the mountain ranges in the southern rift preclude detailed analysis of the timing of episodes of extension and rates of denudation associated with each tectonic event that affected southern New Mexico. Despite the shortcomings of the available data, the results do permit some qualitative analysis.

Laramide deformation

In contrast to data from the northern Rio Grande rift and the Southern Rocky Mountains provinces (Kelley et al., 1992; Kelley and Chapin, 1995), cooling related to Laramide deformation is not well represented in the southern rift AFT data. The preservation in the Sacramento Mountains of a probable uplifted PAZ that formed during Mesozoic burial and the lack of 50 to 70 Ma ages with relatively long mean track lengths like those found in the Front Range of Colorado (Kelley and Chapin, 1995) suggests that Laramide deformation was relatively minor along the eastern margin of the rift. The few minor folds and faults of possible Laramide age that are present in the western escarpment of the Sacramento Mountains apparently did little to disrupt the Mesozoic PAZ. Elsewhere in the southern rift, cooling related to Laramide deformation has been overprinted by later volcanism and extension.

Late Cretaceous to middle Eocene volcanism

Late Cretaceous to Paleocene volcanic centers are rare in central and northern New Mexico. Two acknowledged Laramide-aged intrusive centers in the southern rift are the Salado Hills stock in the Cuchillo Mountains (Chapin et al., 1978) and the Copper Flat stock (Hedlund, 1974) in the Black Range. The identification of a previously unknown Cretaceous intrusion in the Black Range is of interest for two reasons. The first is economic, given the intrusion's proximity to the Copper Flat porphyry copper deposit. Second, the source of the volcanic clasts in the Late Cretaceous to early Tertiary McRae Formation along the eastern flank of the Caballo Mountains has been the subject of some debate (N. McMillan, written comm. 1993). This intrusion (or one like it) appears to be the source for the clasts. Further geochronologic studies on the east side of the Black Range may help identify additional Cretaceous plutons.

Early to middle Eocene volcanism is not common in northern and central New Mexico but is widespread in southern New Mexico and in the Trans-Pecos belt of west Texas. The K-Ar ages for four intrusions in southern New Mexico (Table 3, Fig. 1) and the dikes and sills east of Alamogordo (Asquith, 1974), the 49.6 ±3.8 Ma zircon FT age on the Salinas Peak rhyolite sill in the San Andres Mountains, and the 49.6 ±11.7 Ma age on the probable tuff in the sinkhole near Cloudcroft further establish the limits of Eocene volcanism. The dashed line of Fig. 1 represents the northernmost extent of pre-40 Ma volcanism in south-central New Mexico. As noted by Christiansen and Yeats (1992) and Humphreys (1995), the age of volcanism decreases progressively from 40 to 50 Ma in west Texas, northern Mexico, and southern New Mexico to about 21 Ma in southern Nevada along a west—northwestward trend across the southern Basin and Range province. The new ages help constrain the post-Laramide geometry of the Farallon slab beneath southern New Mexico (Severinghaus and Atwater, 1990; Humphreys, 1995).

Rift extension

The oldest of the four phases of extension is recorded by the low-elevation AFT data in the Sacramento Mountains. Given the preservation of the older AFT ages in the Sacramento Mountains, little denudation is associated with this event. The extensional episodes that began in the late Oligocene and middle Miocene were not observed in the Sacramento Mountains, but waning stages of the late Oligocene episode may be reflected in the cooling history of the Black Mountain stock south of Sierra Blanca. In contrast, cooling related to the earliest phase of extension is not observed in the AFT data from the other mountain ranges in this study; instead the data are dominated by the affects of the late Oligocene and middle Miocene episodes of extension. The cooling rates of 7 to 12°C /m.y. associated with middle Miocene extension in the Organ Mountains imply denudation rates of 200 to 400 m/m.y., assuming a geothermal gradient of 30°C/km. The latest phase of extension, which began in the latest Miocene to Pliocene, is poorly represented in the AFT data because of the lag between the time that cooling commences at depths of 2 to 3 km and the time that the rocks reach the surface. The late Miocene ages in the northern Caballo, Mud Springs, San Andres, and San Diego mountains suggest rapid denudation (250-600 m /m.y.) associated with the latest phase of rifting.

The trend of young AFT ages and greater denudation on the margin of the fault blocks adjacent to the deep side of the half-grabens observed in northern New Mexico is also found in southern New Mexico. For example, using gravity data and limited drill-hole information, Lozinsky and Bauer (1991) found that the Tularosa Basin is underlain by two sub-parallel half-grabens. The eastern half-graben adjacent to the Sacramento Mountains is a relatively shallow bench tilted to the east (maximum of 1200 m of fill). The western half-graben adjacent to the San Andres-Organ Mountains is deeper (at least 1,800 m of fill) and is tilted to the west (Lozinsky and Bauer, 1991). The AFT ages of 7 to 22 Ma are present in the San Andres Mountains adjoining the deep side of the western half-graben. In contrast, the AFT ages are 35 to 112 Ma in the Sacramento Mountains. The AFT data from the Sierra Blanca and Capitan intrusive centers reflect rapid cooling of these shallowly emplaced plutons. In the Palomas Basin, the youngest ages are in the Caballo and Mud Springs Mountains, next to the master fault for the Palomas Basin. Although the AFT age distribution in the Black Range is complex, all of the ages are older than the AFT ages in the Caballo Mountains. Furthermore, the central horst blocks bounded by normal faults on two or three sides, such as San Diego Mountain or the Mud Springs Mountains, have much younger ages than the uplifts on the flanks of the rift.

Comparison of northern and southern rift

Many of the trends observed in the northern Rio Grande rift are also present in the southern rift. As discussed above, the response of the fault blocks adjacent to large faults in the half-grabens that form the Rio Grande rift is similar in both the northern and southern rifts. The cooling of the mountain blocks is controlled by denudation related to flexural isostatic uplift of the fault-bounded ranges (Kelley et al., 1992). Intrarift horst blocks in the southern rift that are bordered by normal faults on two or three sides, like San Diego Mountain or Mud Springs Mountains, invariably have young (<12 Ma) AFT ages and high (>10°C /Ma) cooling rates. In the northern rift, AFT ages of 10 to 20 Ma and rapid cooling rates are commonly associated with blocks bounded on two or more sides by normal faults. Furthermore, in the few places where Mesozoic AFT ages are preserved, the estimated cooling rates are low (<2°C /Ma) in both the northern and southern rift.

Figure 7 summarizes the AFT data from the southern and northern rift. As noted by Chapin (1971) and Baldridge et al. (1983), the Rio Grande rift widens south of the Ladron Mountains. The rift consists of a single half-graben at any given latitude north of the Ladron Mountains, but it is made up of nested or multiple half-grabens to the south. Consequently, the Ladron Mountains were used as the boundary between the northern and southern rifts. The primary difference in the cooling histories of mountain ranges in the northern and southern rift is illustrated in the histograms of Fig. 7. The AFT ages that are older than 30 Ma are more common in the northern Rio Grande rift than they are in the southern rift. Part of this trend may be a function of sampling bias. The southern rift has not been as extensively sampled as the northern rift, and most of the southern-rift samples are from the intrarift horst blocks. Furthermore, the upper parts of the Sacramento, San Andres, and Caballo Mountains are composed primarily of Paleozoic carbonates that lack apatite for AFT dating. If datable rocks were present along the crests of these ranges, older AFT ages like those found in the northern rift would probably be observed. Although part of the trend is related to sampling bias, the combined effects of regional volcanism and greater extension in the southern rift have apparently led to the lack of preservation of ages older than 30 Ma in the southern rift.

The dashed lines in Fig. 7A depict the timing of the initiation of each episode of rifting found in the southern Caballo Mountains. As discussed above, cooling related to the earliest and latest phases of rifting is not well represented in the AFT data, but the late Oligocene and middle Miocene episodes are prominent in Fig. 7A, suggesting that larger amounts of denudation occurred during these phases of extension compared with the earliest episode. Similarly, the rift-related AFT ages from the northern rift cluster in the late Oligocene to middle Miocene range.

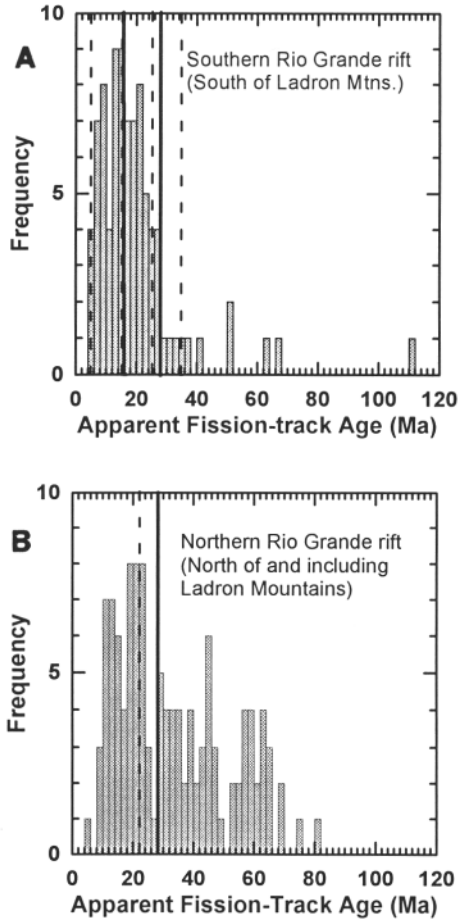

FIGURE 7—Histograms showing the frequency of AFT ages in the (A) southern and (B) northern Rio Grande rift. **A,** AFT ages from central rift south of the Ladron Mountains include data from the Joyita Hills, Lemitar and Magdalena mountains, San Lorenzo Canyon, and the Gonzales prospect (Kelley et. al., 1992). In addition, six unpublished dates from the Lemitar Mountains (9.5 ± 1.8 Ma to 19.7 ± 3.2 Ma) are plotted. Southern rift data are from this study. The dashed lines depict the approximate timing of the beginning of the four extensional episodes in the southern rift proposed by Mack et al. (1994a, b). The solid lines are the times of major episodic extension in the Lemitar Mountains (Cather et al., 1994). **B,** AFT ages north of and including the Ladron Mountains from Kelley et al. (1992) and sources therein. Central rift data include AFT ages from the Sandia, Manzano, Los Pinos, and Ladron Mountains. Solid line represents the earliest onset of extension in the northern rift, and the dashed line represents the oldest dated volcanic rock interbedded with basin-fill sediments in the Albuquerque Basin (Chapin and Cather, 1994).

Love Ranch clasts

The original intent of this part of the investigation was to try to put constraints on the age of the Love Ranch Formation. Unfortunately, the AFT results do nothing to clarify the age of the Love Ranch; however, the data can be used to address the thermal history of the southern Jornada del Muerto. The AFT ages of three granitic clasts from the Love Ranch Formation range from 13.2 ±3.1 Ma to 22.7 ±0.9 Ma, significantly younger than the stratigraphic age of the unit. The spread in ages may be related to differences in apatite composition among the clasts. The high-mean-track lengths for these samples indicate that the clasts were heated to temperatures above 120°C following deposition in the basin, completely annealing pre-existing fission tracks. Heating of the samples occurred during burial by about 2 km of volcanic and volcaniclastic rocks in a part of the Jornada del Muerto that has elevated heat flow (115-127 mW / m^2; Reiter and Barroll, 1990). The samples subsequently cooled relatively rapidly during exhumation in the early to middle Miocene.

Conclusions

1. The AFT data from the Caballo, Mud Springs, San Diego, and Doña Ana mountains and the sedimentologic data from the Oligocene to Miocene Hayner Ranch and Rincon Valley Formations (Mack et al., 1994a, b) are consistent.

2. The 21 to 22 Ma AFT ages in the Proterozoic rocks on the east side of the San Andres Mountains record cooling in response to the phase of extension that began in the late Oligocene. Younger AFT ages of 7 to 8 Ma related to the middle Miocene episode of extension are exposed on the upthrown side of high-angle faults cutting the Proterozoic rocks.

3. The AFT ages from the eastern Organ Mountains are 10 to 17 Ma and the mean track lengths are long; the ages on the west side are 20 to 29 Ma and the mean track lengths are shorter. A westward-tilted partial-annealing zone for apatite that formed during protracted cooling of the Organ batholith in the early Miocene to late Oligocene is preserved in this mountain block. Rapid denudation (200-400 m/m.y.) and tilting of the range occurred in the middle Miocene.

4. The base of a poorly defined apatite partial-annealing zone that formed during Mesozoic burial of southern New Mexico is preserved in the Sacramento Mountains. The earliest phase of extension is recorded in the AFT data from Proterozoic rocks exposed at the base of the Sacramento escarpment. Evidence for significant denudation related to Laramide deformation, or late Oligocene and middle Miocene extension is not observed in the AFT data.

5. The AFT data derived from samples in Oligocene to Miocene intrusions (Capitan, Sierra Blanca, and Black Range) record rapid cooling of these shallowly emplaced plutons.

6. The AFT data from the northern and southern Rio Grande rift are similar in many respects. The trend of young AFT ages and greater denudation on the margin of fault blocks adjacent to the master faults controlling the geometry of the half-grabens that was observed in northern New Mexico is also found in southern New Mexico. Horst blocks in the rift that are bordered by normal faults on two or three sides invariably have young (<12 Ma) AFT ages and high (>10°C /Ma) cooling rates. In the places where Mesozoic AFT ages are preserved, the estimated cooling rates are low (<2°C /Ma) in both the northern and southern rift. The primary difference in the cooling histories of mountain ranges in the northern and southern rift is the paucity of AFT ages that are older than 30 Ma in the southern rift. Part of this trend may be a function of sampling bias.

7. A previously unrecognized Cretaceous intrusion was identified southeast of Hillsboro using zircon FT dating. The porphyry from this intrusion was the source of volcanic clasts in the Late Cretaceous to early Tertiary McRae Formation located in the northeastern Caballo Mountains.

8. A zircon FT age of 49.6 ±3.8 Ma on the rhyolite sill exposed on Salinas Peak at the north end of the San Andres Mountains and K-Ar ages of the Orogrande, Cuchillo, and Tres Hermanos stocks constrain the northern limit of pre-40 Ma volcanism in south-central New Mexico.

ACKNOWLEDGMENTS—This project was supported by NSF grant EAR8804203 and by the New Mexico Bureau of Mines and Mineral Resources. Thanks to William Seager for donating some of his samples from the Organ batholith and for his help in collecting samples in the San Andres Mountains. Sam Seek helped us gain access to the San Andres Mountains on White Sands Missile Range, and range riders Rod Pino and Chris Ortega provided transportation during our visit. Paul Bauer collected the Proterozoic samples from the Sacramento Mountains. Pam Roths provided samples from the Little San Nicolas and Dead Man Canyon areas in the San Andres Mountains and from the Franklin Mountains. Thanks to Nancy McMillan for her discussions concerning the McRae Formation. The samples were irradiated under the DOE reactor share program at the Texas A&M Nuclear Science Center. We appreciate the constructive reviews of Greg Mack and an anonymous reviewer.

References

Abitz, R. J., 1986, Geology of mid-Tertiary volcanic rocks of the east-central Black Range, Sierra County, New Mexico: Implications for a double cauldron complex in the Emory cauldron; *in* Clemons, R. E., King, W. E., Mack, G. H., and Zidek, J. (eds.), Truth or Consequences Region: New Mexico Geological Society, Guidebook 37, pp. 161-166.

Allen, M. S., and Foord, E. E., 1991, Geological, geochemical and isotopic characteristics of the Lincoln County porphyry belt, New Mexico: implications for regional tectonics and mineral deposits; *in* Barker, J. M., Kues, B. S., Austin, G. S., and Lucas, S. G. (eds.), Geology of the Sierra Blanca, Sacramento, and Capitan Ranges, New Mexico: New Mexico Geological Society, Guidebook 42, pp. 97-102..

Allen, M. S., and McLemore, V. T., 1991, The geology and petrogenesis of the Capitan pluton, New Mexico; *in* Barker, J. M., Kues, B. S., Austin, G. S., and Lucas, S. G. (eds.), Geology of the Sierra Blanca, Sacramento, and Capitan Ranges, New Mexico: New Mexico Geological Society, Guidebook 42, pp. 115-128.

Asquith, G. B., 1974, Petrography and petrogenesis of Tertiary camptonites and diorites, Sacramento Mountains, New Mexico: New Mexico Bureau of Mines and Mineral Resources, Circular 141, 6 pp.

Baldridge, W. S., Bartov, Y., and Kron, A., 1983, Geologic map of the Rio Grande rift and southeastern Colorado Plateau, New Mexico and Arizona; *supplement to* Riecker, R. E. (ed.), Rio Grande Rift: Tectonics and Magmatism: Washington, D.C., American Geophysical Union, scale 1:500,000.

Bowsher, A. L., 1991, Some effects of Precambrian basement on the development of the Sacramento Mountains; *in* Barker, J. M., Kues, B. S., Austin, G. S., and Lucas, S. G. (eds.), Geology of the Sierra Blanca, Sacramento, and Capitan Ranges, New Mexico: New Mexico Geological Society, Guidebook 42, pp. 81-89.

Campbell, A. R., Heizler, M. T., and Dunbar, N. W., 1994, $^{40}Ar/^{39}Ar$ dating of fluid inclusions in quartz from the Capitan pluton, New Mexico (abs.): PACROFI, v. 5, p. 11.

Carlson, W. D., 1990, Mechanisms and kinetics of apatite fission-track annealing: American Mineralogist, v. 75, pp. 1120-1139.

Cather, S. M., Chamberlin, R. M., Chapin, C. E., and McIntosh, W. C., 1994, Stratigraphic consequences of episodic extension in the Lemitar Mountains, central Rio Grande rift; *in* Keller, G. R., and Cather, S. M. (eds.), Basins of the Rio Grande Rift: Structure, Stratigraphy, and Tectonic Setting: Geological Society of America, Special Paper 291, pp. 157-170.

Chapin, C. E., 1971, The Rio Grande rift, pt. 1: modifications and additions; *in* James, H. L. (ed.), San Luis Basin (Colorado): New Mexico Geological Society, Guidebook 22, pp. 191-201.

Chapin, C. E., and Cather, S. M., 1994, Tectonic setting of the axial basins of the northern and central Rio Grande rift; *in* Keller, G. R., and Cather, S. M. (eds.), Basins of the Rio Grande Rift: Structure, Stratigraphy, and Tectonic Setting: Geological Society of America, Special Paper 291, pp. 5-25.

Chapin, C. E., Chamberlin, R. M., Osburn, G. R., Sanford, A. R., and White, D. W., 1978a, Exploration framework of the Socorro geothermal area, New Mexico; *in* Chapin, C. E., Elston, W. E., and James, H. L. (eds.), Field guide to selected cauldrons and mining districts of the Datil-Mogollon volcanic field, New Mexico: New Mexico Geological Society, Special Publication 7, pp. 115-130.

Chapin, C. E., Jahns, R. H., Chamberlin, R. M., and Osburn, G. R., 1978b, First-day road log from Socorro to Truth or Consequences via Magdalena and Winston; *in* Chapin, C. E., Elston, W. E., and James, H. L. (eds.), Field guide to selected cauldrons and mining districts of the Datil-Mogollon volcanic field, New Mexico: New Mexico Geological Society, Special Publication 7, pp. 1-31.

Christiansen, R. L., and Yeats, R. L., 1992, Post-Laramide geology of the U.S. Cordilleran region; *in* Burchfiel, B. C., et al. (eds.), The Cordilleran Orogen: Conterminous U.S.: Geological Society of America, Geology of North America, v. G-3, pp. 261-406.

Clemons, R. E., and Osburn, G. R., 1986, Geology of the Truth or Consequences area; *in* Clemons, R. E., King, W. E., Mack, G. H., and Zidek, J. (eds.), Truth or Consequences Region: New Mexico Geological Society, Guidebook 37, pp. 69-81.

Corrigan, J. D., 1991, Deriving thermal history information from apatite fission-track data: Journal of Geophysical Research, v. 96, pp. 10,347-10,360.

Elston, W. E., 1989, Day 5: Field guide to the Emory caldera along NM-152 and in Tierra Blanca Canyon: New Mexico Bureau of Mines and Mineral Resources, Memoir 46, pp. 91-106.

Fitzgerald, P. G., Sorkhabi, R. B., Redfield, T. F., and Stump, E., 1995, Uplift and denudation of the central Alaska Range: a case study in the use of apatite fission-track thermochronology to determine absolute uplift parameters: Journal of Geophysical Research, v. 100, pp. 20,175-20,191.
Foster, D. A., and Gleadow, A. J. W., 1992, The morpho-tectonic evolution of rift-margin mountains in central Kenya: constraints from apatite fission-track thermochronology: Earth and Planetary Science Letters, v. 113, pp. 157-171.

Gleadow, A. J. W., and Fitzgerald, P. F., 1987, Uplift history and structure of the Transantarctic Mountains: new evidence from fission track dating of basement apatites in the Dry Valleys area, southern Victoria Land: Earth and Planetary Science Letters, v. 82, pp. 1-14.

Green, P. F., 1985, A comparison of zeta calibration baselines in zircon, sphene, and apatite: Chemical Geology (Isotope Geoscience Section), v. 58, pp. 1-22.

Green, P. F., Duddy, I. R., Gleadow, A. J. W., Tingate, P. R., and Laslett, G. M., 1986, Thermal annealing of fission tracks in apatite, 1. A qualitative description: Chemical Geology (Isotope Geoscience Section), v. 59, pp. 237-253.

Green, P. F., Duddy, I. R., Laslett, G. M., Hegarty, K. A., Gleadow, A. J. W., and Lovering, J. F., 1989, Thermal annealing of fission tracks in apatite, 4. Quantitative modeling techniques and extension to geological timescales: Chemical Geology (Isotope Geoscience Section), v. 79, pp. 155-182.

Hedlund, D. L., 1974, Age and structural setting of base-metal mineralization in the Hillsboro-San Lorenzo area, southwestern New Mexico; *in* Siemers, C. T., Woodward, L. A., and Callender, J. F. (eds.), Ghost Ranch: New Mexico Geological Society, Guidebook 25, pp. 378-379.

Humphreys, E. D., 1995, Post-Laramide removal of the Farallon slab, western United States: Geology, v. 23, pp. 987-990.

Hurford, A. J., 1986, Cooling and uplift patterns in the Lepontine Alps, south central Switzerland and an age of vertical movement on the Insubric fault line: Contributions to Mineralogy and Petrology, v. 92, pp. 413-427.

Hurford, A. J., and Green, P. F., 1983, The zeta age calibration of fission-track dating: Chemical Geology (Isotope Geoscience Section), v. 1, pp. 285-317.

Keller, G. R., Morgan, P., and Seager, W. R., 1990, Crustal structure, gravity anomalies and heat flow in the southern Rio Grande rift and their relationship to extensional tectonics: Tectonophysics, v. 174, pp. 21-37.

Kelley, S. A., and Chapin, C. E., 1995, Apatite fission-track thermochronology of Southern Rocky Mountain-Rio Grande rift-western High Plains provinces; *in* Bauer, P. W., Kues, B. S., Dunbar, N. W., Karlstrom, K. E., and Harrison, B. (eds.), Geology of the Santa Fe Region: New Mexico Geological Society, Guidebook 46, pp. 87-96.

Kelley, S. A., Chapin, C. E., and Corrigan, J., 1992, Late Mesozoic to Cenozoic cooling histories of the flanks of the northern and central Rio Grande rift, Colorado and New Mexico: New Mexico Bureau of Mines and Mineral Resources, Bulletin 145,39 pp.

Laslett, G. M., Kendall, W. S., Gleadow, A. J. W., and Duddy, I. R., 1982, Bias in measurement of fission-track length distribution: Nuclear Tracks, v. 6, p. 79-85.

Lozinsky, R. P., and Bauer, P. W., 1991, Structure and basin fill units of the Tularosa Basin; *in* Barker, J. M., Kues, B. S., Austin, G. S., and Lucas, S. G. (eds.), Geology of the Sierra Blanca, Sacramento, and Capitan Ranges, New Mexico: New Mexico Geological Society, Guidebook 42, pp. 7-9.

Lozinsky, R. P., and Hawley, J. W., 1986, Upper Cenozoic Palomas Formation of south-central New Mexico; *in* Clemons, R. E., King, W. E., Mack, G. H., and Zidek, J. (eds.), Truth or Consequences Region: New Mexico Geological Society, Guidebook 37, pp. 239-247.

Mack, G. H., and Seager, W. R., 1990, Tectonic control on facies distribution of the Camp Rice and Palomas Formations (Plio-Pleistocene) in the southern Rio Grande rift: Geological Society of America, Bulletin, v. 102, pp. 45-53.

Mack, G. H., Seager, W. R., and Kieling, J., 1994a, Late Oligocene and Miocene faulting and sedimentation, and evolution of the southern Rio Grande rift, New Mexico: Sedimentary Geology, v. 92, pp. 79-96.

Mack, G. H., Nightengale, A. L., Seager, W. R., and Clemons, R. E., 1994b, The Oligocene Goodsight-Cedar Hills half-graben near Las Cruces and its implication to the evolution of the Mogollon-Datil volcanic field and to the southern Rio Grande rift; *in* Chamberlin, R. M., Kues, B. S., Cather, S. M., Barker, J. M., and McIntosh, W. C. (eds.), Mogollon Slope: New Mexico Geological Society, Guidebook 45, pp. 135-142.

Maggiore, P., 1981, Deformation and metamorphism in the floor of a major ash-flow cauldron, the Emory cauldron, Grant and Sierra Counties, New Mexico: Unpublished MS thesis, University of New Mexico, Albuquerque, 133 pp.

McIntosh, W. C., Chapin, C. E., Ratte, J. C., Sutter, J. F., 1992a, Time-stratigraphic framework of the Eocene-Oligocene Mogollon-Datil volcanic field, southwestern New Mexico: Geological Society of America, Bulletin, v. 104, pp. 851-871.

McIntosh, W. C., Geissman, J. W., Chapin, C. E, Kunk, M. J., and Henry, C. D., 1992b, Calibration of the latest Eocene-Oligocene geomagnetic polarity time scale using $^{40}Ar/^{39}Ar$ dated ignimbrites: Geology, v. 20, pp. 459-463.

Moore, S. L., Thompson, T. B., and Foord, E. E., 1991, Structure and igneous rocks of the Ruidoso region, New Mexico; *in* Barker, J. M., Kues, B. S., Austin, G. S., and Lucas, S. G. (eds.), Geology of the Sierra Blanca, Sacramento, and Capitan Ranges, New Mexico: New Mexico Geological Society, Guidebook 42, pp. 137-145.

Naeser, C. W., 1979, Fission-track dating and geologic annealing of fission tracks; *in* Jager, E., and Hunziker, J. C. (eds.), Lectures in Isotope Geology: Springer-Verlag, New York, pp. 154-169.

Roths, P., 1991, Geology of Proterozoic outcrops in Dead Man and Little San Nicolas Canyons, southern San Andres Mountains, New Mexico; *in* Barker, J. M., Kues, B. S., Austin, G. S., and Lucas, S. G. (eds.), Geology of the Sierra Blanca, Sacramento, and Capitan Ranges, New Mexico: New Mexico Geological Society, Guidebook 42, pp. 91-96.

Reiter, M., and Barroll, M. W., 1990, High heat flow in the Jornada del Muerto: a region of crustal thinning in the Rio Grande rift without upper crustal extension: Tectonophysics, v. 174, pp. 183-195.

Reiter, M., Shearer, C., Edwards, C. L., 1978, Geothermal anomalies along the Rio Grande rift in New Mexico: Geology, v. 6, pp. 85-88.

Reiter, M., Eggleston, R. E., Broadwell, B. R., and Minier, J., 1986, Estimates of terrestrial heat flow from deep petroleum tests along the Rio Grande rift in central and southern New Mexico: Journal of Geophysical Research, v. 91, pp. 6225-6245.

Seager, W. R., 1981, Geology of the Organ Mountains and southern San Andres Mountains, New Mexico: New Mexico Bureau of Mines and Mineral Resources, Memoir 36,97 pp.

Seager, W. R., 1986, Third-day road log from Truth or Consequences to southeastern Caballo Mountains and San Diego Mountain via 1-25 and the Jornada del Muerto; *in* Clemons, R. E., King, W. E., Mack, G. H., and Zidek, J. (eds.), Truth or Consequences Region: New Mexico Geological Society, Guidebook 37, pp. 35-52.

Seager, W. R., and Clemons, R. E., 1975, Middle to late Tertiary geology of the Cedar Hills-Selden Hills area, New Mexico: New Mexico Bureau of Mines and Mineral Resources, Circular 133, 24 pp.

Seager, W. R., and Mack, G. H., 1986, Laramide paleotectonics of southern New Mexico; *in* Peterson, J. A. (ed.), Paleotectonics and Sedimentation in the Rocky Mountain Region: American Association of Petroleum Geologists, Memoir 41, pp. 669-685.

Seager, W. R., and McCurry, M., 1988, The cogenetic Organ cauldron and batholith, south-central New Mexico, evolution of a large-volume ash-flow cauldron and its source magma chamber: Journal of Geophysical Research, v. 93, pp. 4421-4433.

Seager, W. R., Clemons, R. E., Hawley, J. W., and Kelley, R. E., 1982, Geology of the northwest part of the Las Cruces 1°x2° sheet, New Mexico: New Mexico Bureau of Mines and Mineral Resources, Geologic Map 53, scale 1:125,000.

Seager, W. R., Mack, G. H., Raimonde, M. S., and Ryan, R. G., 1986, Laramide basement-cored uplift and basins in south-central New Mexico; *in* Clemons, R. E., King, W. E., Mack, G. H., and Zidek, J. (eds.), Truth or Consequences Region: New Mexico Geological Society, Guidebook 37, pp. 123-130.

Seager, W. R., Shafiqullah, M., Hawley, J. W., and Marvin, R. F., 1984, New K-Ar dates from basalts and the evolution of the southern Rio Grande rift: Geological Society of America, Bulletin, v. 95, pp. 87-99.

Severinghaus, J., and Atwater, T., 1990, Cenozoic geometry and thermal state of the subducting slabs beneath western North America; *in* Wernicke, B. P. (ed.), Basin and Range Extension Tectonics near the Latitude of Las Vegas, Nevada: Geological Society of America, Memoir 176, pp. 1-22.

Swisher, C. C., and Prothro, D. R., 1990, Single-crystal $^{40}Ar/^{39}Ar$ dating of the Eocene-Oligocene transition in North America: Science, v. 249, pp. 760-762.

Thompson, T. B., 1972, Sierra Blanca igneous complex, New Mexico: Geological Society of America, Bulletin, v. 83, pp. 2341-2356.

Woodward, L. A., Callender, J. F., Seager, W. R., Chapin, C. E., Gries, J. C., Shaffer, W. L., and Zilinski, R. E., 1978, Tectonic map of the Rio Grande rift region in New Mexico, Chihuahua, and Texas: New Mexico Bureau of Mines and Mineral Resources, Circular 163, Sheet 2. ❑